LA-UR-17-23190
Approved for public release; distribution is unlimited.

Title: Assessment of Laser-Driven Pulsed Neutron Sources for Poolside Neutron-based Advanced NDE – A Pathway to LANSCE-like Characterization at INL

Author(s): Roth, Markus
Vogel, Sven C.
Bourke, Mark Andrew M.
Fernandez, Juan Carlos
Mocko, Michael Jeffrey
Glenzer, Siegfried
Leemans, Wim
Siders, Craig
Haefner, Constantin

Intended for: Report

Issued: 2017-04-19

Assessment of Laser-Driven Pulsed Neutron Sources for Poolside Neutron-based Advanced NDE – A Pathway to LANSCE-like Characterization at INL

Nuclear Technology Research and Development

Prepared for
U.S. Department of Energy
Nuclear Technology Research and Development Program
Advanced Fuels Campaign

M. Roth[1], S. C. Vogel[2], M. A. M. Bourke[2], J. Fernandez[2], M. Mocko[2], S. Glenzer[3], W. Leemans[4], C.W. Siders[5], C. Haefner[5]
[1]TU Darmstadt/Germany, [2]LANL, [3]Stanford University, [4]LBNL, [5]LLNL

April 14, 2017
NTRD-FUEL-2017-000064

SUMMARY

A variety of opportunities for characterization of fresh nuclear fuels using thermal (~25meV) and epithermal (~10eV) neutrons have been documented at Los Alamos National Laboratory. They include spatially resolved non-destructive characterization of features, isotopic enrichment, chemical heterogeneity and stoichiometry. The LANSCE spallation neutron source is well suited in neutron fluence and temporal characteristics for studies of fuels. However, recent advances in high power short pulse lasers suggest that compact neutron sources might, over the next decade, become viable at a price point that would permit their consideration for poolside characterization on site at irradiation facilities.

In a laser-driven neutron source the laser is used to accelerate deuterium ions into a beryllium target where neutrons are produced. At this time, the technology is new and their total neutron production is approximately four orders of magnitude less than a facility like LANSCE. However, recent measurements on a sub-optimized system demonstrated $>10^{10}$ neutrons in sub-nanosecond pulses in predominantly forward direction. The compactness of the target system compared to a spallation target may allow exchanging the target during a measurement to e.g. characterize a highly radioactive sample with thermal, epithermal, and fast neutrons as well as hard X-rays, thus avoiding sample handling. At this time several groups are working on laser-driven neutron production and are advancing concepts for lasers, laser targets, and optimized neutron target/moderator systems. Advances in performance sufficient to enable poolside fuels characterization with LANSCE-like fluence on sample within a decade may be possible.

This report describes the underlying physics and state-of-the-art of the laser-driven neutron production process from the perspective of the DOE/NE mission. It also discusses the development and understanding that will be necessary to provide customized capability for characterization of irradiated fuels. Potential operational advantages compared to a spallation neutron source include reduced shielding complexity, reduced energy requirements, and a production target free of fission products. Contributors to this report include experts in laser-driven neutron production (Roth, Fernandez), laser design (Haefner, Siders, Leemans), laser target design (Glenzer), spallation target/moderator design (Mocko), neutron instrumentation and characterization applications (Vogel, Bourke).

CONTENTS

SUMMARY iii

ACRONYMS x

1. INTRODUCTION 1

2. Present neutron use and need for small & medium scale facilities 3

3. State of the art 5
   - 3.1 Lasers 5
   - 3.2 Neutron Sources 7

4. Laser driven particle accelerators 8
   - 4.1 Photon induced reactions 9
   - 4.2 Cluster fusion 10

5. Laser-driven ion acceleration 11
   - 5.1 Target Normal Sheath Acceleration 11
   - 5.2 Other Particle Acceleration Mechanisms 13
   - 5.3 Neutron producing reactions 14
   - 5.4 Neutron production 15

6. Prospects 19

7. Novel Cryogenic Deuterium Jet Targets for Laser Neutron Sources 21
   - 7.1 Cryogenic Laser proton source and deuteron acceleration system 22
   - 7.2 Simulations 26

8. A “Laser-LANSCE” Facility 27
   - 8.1 Overview of LANSCE 27
   - 8.2 Thermal neutrons for material characterization 28
   - 8.3 Epithermal neutrons for material characterization and cross-section measurements 28
   - 8.4 MeV neutron and X-ray Flash Radiography 30
   - 8.5 Protons for material characterization 31
   - 8.6 Isotope production and proton irradiation 32

9. Comparison to the field 32

10. Other Applications 35
    - 10.1 Fast neutron radiography 35
    - 10.2 Active Interrogation of Sensitive Nuclear Material 36
    - 10.3 On-site neutron based system tests 36
    - 10.4 Radiation Damage Research 36
    - *10.5* Academic Access 37

11. World-wide Research Activities in Laser-driven Neutron Sources 37

12. Summary and Outlook... 39

13. References 41

FIGURES

Figure 1: Three pillars of the LANL Advanced Non-destructive Evaluation and Advanced Post-irradiation Examination program.. 3

Figure 2: Characterization of three ceramic fuel pellets with different enrichment levels using computer tomography reconstruction of isotope specific densities. The agreement of nominal and measured enrichment is within ~0.1%... 4

Figure 3: Characterization of a U-10 wt%Zr transmutation fuel with 5 wt% rare earth element inclusions. The thermal CT allows to measure gaps between the inner and outer container as well as fuel and container. However, inclusions are only visible as inhomogeneities whereas the ability to visualize locations of ^{145}Nd and ^{238}U atoms allows to unambiguously identify them as rare earth agglomerates [Vogel 2016a]........ 5

Figure 4: History of high power lasers. Left: Peak power versus year. The large jump in peak power in the late 1990's was achieved by the Livermore Petawatt Laser and over the next decade and a half duplicated by dozens of facilities globally. The late 2010's anticipate a second leap in peak power with the commissioning of several 10-PW class lasers currently under construction. Center: Peak focal intensity (reported) versus year, showing a similarly punctuated equilibrium evolution in peak intensity. Interestingly, during the 15-year „PW Plateau“, peak reported intensities increased as rep-rate and active wavefront control improved the focusability of PW peak powers (right). The late 2010's will also show the commissioning of high rep-rate (10-Hz in the case of the HAPLS system) PW lasers, which are anticipated to achieve true diffraction limited intensities of 10^{23} W/cm^2 which have eluded PW system builders for two decades. Figures used with permission from C.W. Siders and C. Haefner, Nuclear Photonics 2016, Monterey CA. 6

Figure 5: Historic development of thermal neutron flux [CSNS 2017]for comparison with the laser intensity evolution in Figure 4, center, and evolution of laser-driven neutron production in Figure 15. The 10^{10} n/pulse achieved at Trident place the development of laser-driven neutron sources approximately at the first spallation neutron source ZING-P (with the considerations about number of neutrons reaching a moderator described in the text)... 8

Figure 6: Energy dependent cross section for photonuclear (γ,xn) reactions for different isotopes (from [Guenther 2011]). 10

Figure 7: Target Normal Sheath Acceleration – TNSA. A thin target foil with the thickness d=5-50 µm is irradiated by an intense laser pulse. The laser pre-pulse creates a pre-plasma on the target's front side. The main pulse interacts with the plasma and accelerates MeV-energy electrons mainly in the forward direction. The electrons propagate through the target, where collisions with the background material can increase the divergence of the electron current. The electrons leave the target, resulting in a dense sheath. An electric field due to charge separation is created. The field is of the order of laser's

electric field (TV/m), which ionizes atoms at the surface. The ions are then accelerated in this field, pointing in the target normal direction. 12

Figure 8: typical pitcher-catcher geometry for laser driven neutron production using ion beams. 14

Figure 9: Neutron yield for deuteron induced reactions in an infinite catcher geometry (data from McMahan et al., Neutron beams from deuteron breakup at the 88-inch cyclotron, Int. Conf. on Nucl. Data for Science and Technology 2007).. 15

Figure 10: Simulated neutron production efficiencies per ion for different catcher isotopes assuming a typical, laser-driven ion energy spectrum (as observed with the Phelix laser). Simulations performed using GEANT4.. 16

Figure 11: typical proton spectrum of an ultra-intense laser.. 17

Figure 12: Energy-dependent proton and deuteron induced neutron production using 10^{13} ions from a typical laser source at a cutoff energy around 25 MeV/u. (like in Figure 11) ... 18

Figure 13 Target thickness sensitivity and directionality of the neutron emission based on ion beams accelerated in the relativistic transparency regime. 19

Figure 14: Schematic of the LANSCE target-moderator-reflector-shielding (TMRS) system. The water moderators are shown in red with the stack of tungsten disks shown in blue being the spallation target [Mocko 2013]. 20

Figure 15: Laser driven neutron numbers versus laser intensity. The neutron numbers of the directed neutron beam are compared to a conventional isotropic neutron source. Results in red indicate short pulse lasers below 100 fs, blue are high energy lasers around 0.5 ps pulse duration and the yellow marks indicate the prospect for upcoming systems currently under construction. 21

Figure 16: Results from 3-D particle in cell simulations using the code OSIRIS show the production of a high-energy proton pulse. These simulations indicate the hydrogen jet in blue, the laser in green, and protons in orange-red. At the end of the 50fs-long laser pulse, a pure energetic proton beam with 10^{10} particles emanates from the target. The proton beam energy of 20 MeV and its normalized emittance 0.1 mm-mrad meet requirements for injection and acceleration with a high-gradient rf accelerator. 23

Figure 17: Stanford's continuously flowing cryogenic hydrogen micro-jet for laser-driven plasma acceleration experiments (LCLS experiment 2015). (Top left) Image of a 150 mJ, 45 fs laser beam interacting with the jet is shown. The laser was focused to a 4 µm laser focal spot hitting the target at 1 Hz. (Top right) The jet's spatial stability has been measured with shadowgraphy and the data shown on the bottom right indicate stability of 1 µm rms. (Bottom left) The jet density profile has been measured in situ with a probe laser using interferometry. 24

Figure 18: The experimental setup of a proton acceleration experiment using cryogenic micro-jets target is shown. A 4 J, 30 fs high-intensity laser pulse is focused on the micro-jet using a mixture of hydrogen and deuterium. The laser-driven proton and deuteron beam is investigated using a radiochromic film (RCF) stack, Thomson parabola spectrometers and Be converter with a multi-channel-plates (MCP) for neutron radiography. The Thomson parabola data are an example from an experiment at Titan. 25

Figure 19: Proton spectra are shown from cryogenic hydrogen measured for 60 seconds and at 1 Hz. This target allows achieving high dose. 25

Figure 20: Proton spectra from the interaction of a 4 J, 50 fs, $8x10^{20}$ W/cm^2 laser with a hydrogen target with thickness of 1 µm (red) and 5 µm (blue). The number of protons with 20±1 MeV is ~ 10^{10} (red) and $2x10^9$ (blue). 27

Figure 21: Photograph of the setup for demonstration experiment at the Trident source (left) and single pulse radiograph (right). The attenuation of the polyethylene step wedge in the bottom left indicates that the radiation is predominantly neutrons (Radiograph courtesy of R. Nelson & J. Hunter/LANL). 30

Figure 22: Comparison of an AWE tungsten kaleidoscope used to determine resolution in radiography experiments. On the left, a radiograph from the Dual Axis Radiographic Hydrodynamic (DARHT) facility is shown. On the right, the same target is shown with a radiograph measured at Trident (Radiographs courtesy of R. Nelson & J. Hunter/LANL). 31

Figure 23: Comparison of mock-up fuel pellets used in [Morris 2013] and [Tremsin 2013]. The pellets contained purposefully introduced flaws and tungsten inclusions, which are only visualized by the energy-resolved epi-thermal neutron imaging. 32

Figure 24: Example of laser-driven fast neutron radiography. The tungsten blocks in front of the detector result in absorption and scattering of the neutrons shown in intensity variations in the scintillating fiber detector. This image was taken without neutron energy selection (in contrast to [Roth 2013]) 35

Figure 25: Conference attendees of the Nuclear Photonics conference in Monterey, CA, October 2016. Several authors of this report were in the attendance, author M. Roth served as program chair for the conference. 38

TABLES

Table 1: Comparison of different neutron sources. 34

ACRONYMS

ANDE	Advanced Non-destructive Examination
ATR	Advanced Test Reactor
AWE	Atomic Weapons Establishment
BOA	Break-out Afterburner
CSNS	Chinese SNS
CT	Computed Tomography
DARHT	Dual Axis Radiographic Hydrodynamic Test Facility
DOE/NE	Department of Energy/Nuclear Energy program
ESS	European Spallation Source
ELI	Extreme Light Infrastructure
FP5	Flight-path 5 (imaging beam line at LANSCE)
GSI	Gesellschaft für Schwerionenforschung (Society for Heavy Ion Research)
HIPPO	High-Pressure/Preferred Orientation (diffractometer at LANSCE)
INL	Idaho National Laboratory
LANL	Los Alamos National Laboratory
LANSCE	Los Alamos Neutron Science Center
LCLS	Linac Coherent Light Source
Linac	Linear Accelerator
MCP	Multi-channel plate
NRTA	Neutron Resonance Transmission Analysis
ORNL	Oak Ridge National Laboratory
RCF	Radiochromic Film
SLAC	Stanford Linear Accelerator Center
SNS	Spallation Neutron Source (at ORNL)
TMRS	Target-moderator-reflector-system
TNSA	Target normal sheath acceleration

POTENTIAL OF POOLSIDE LANSCE-LIKE NEUTRON CHARACTERIZATION CAPABILITIES WITH LASER-DRIVEN NEUTRON SOURCES

1. INTRODUCTION

Neutron sources applicable to research, interrogation, or irradiation are at present either large scale reactor or spallation neutron user facilities or small accelerator based sources with fluxes prohibitive for diffraction or cross-section measurements for example. The confluence of recent developments in diverse areas brings within reach of present technology laser-driven pulsed neutron sources with neutron fluxes comparable to those of state-of-the-art user facilities. These diverse areas include intense, pulsed lasers [Dawson 2012], increase in laser pulse contrast ("pulse cleaning") [Shah 2009], and new insights into the underlying physics of laser-driven neutron generation, e.g. the so-called break-out afterburner (BOA) laser-driven ion-acceleration mechanism predicted on the Roadrunner supercomputer at Los Alamos [Yin 2006, Yin 2007] and later experimentally confirmed with the Trident laser at LANL [Fernandez 2017] and the Phelix laser at GSI in Germany. BOA has been instrumental in a quantum leap in laser-driven neutron-beam generation performance [Roth 2013, Alejo 2016, Fernandez 2017]. Compared to the multi-billion dollar investment required for a modern neutron user facility (e.g. $1.4B for the SNS [Day 2011], $1.4B for the SNS second target station [SNS 2017], or €1.843 billion for the ESS projects [ESS 2014]), laser-driven neutron sources would require investments likely between one or two orders of magnitude smaller while providing comparable source characteristics and much smaller operational cost. Furthermore, the real estate footprint of such a source would be a large room rather than a kilometer long accelerator or a full nuclear reactor, which reduces the investment cost and enables even mobile facilities. This potentially would provide dedicated and affordable sources to facilities and organizations with specific needs, such as material characterization (e.g. material science applications) or interrogation (e.g. nuclear contraband detection). From the viewpoint of non-proliferation, laser-driven neutron sources could provide comparable research capabilities in some fields as research reactors, but without the need to distribute and track nuclear fuels or monitor e.g. breeding activities.

As discussed below, due to technical limitations with spallation targets or reactor cores, potential increases in thermal neutron flux for next-generation neutron sources are at best an order of magnitude over decades. In contrast, laser intensity, a critical performance factor (but not exclusive) in laser-driven neutron generation, has increased and is still increasing by several orders of magnitude per decade. Current understanding of the physics predict linear or better coupling between neutron output efficiency and laser intensity, hence providing a new avenue to build large scale neutron facilities surpassing the presently available neutron fluxes at much reduced investment cost in the future. For small scale applications such as characterization tools, the secular increase in laser intensity may allow increased neutron fluxes at laser-driven installations via upgraded laser systems while keeping target/moderator and detector systems, adding to the economic attractiveness of such a system.

Recently, record-setting neutron fluxes of 10^{10} n/pulse were demonstrated by our team at the ~80J Trident laser facility at LANL [Roth 2013]. Due to the target design for those experiments (described below), with a moderator surrounding the beryllium target producing predominantly forward traveling neutrons, the vast majority of the laser-produced neutrons are injected into the moderator. For comparison, based on estimates detailed in section 6, at LANSCE 2×10^{13} n/pulse reach the moderator serving two diffraction and an imaging beamline. Concepts exists to reach or exceed these numbers with a laser-driven neutron source, e.g. with target optimizations or application of laser sources with existing technology to provide higher energy than Trident. A laser-driven neutron source on par with LANSCE is therefore within reach and groups all over the world are working towards this goal with various applications in mind (section

11). As neutrons may be produced by deuteron break-up rather than spallation, which has been demonstrated with low-Z elements such as beryllium, much less radioactive inventory is produced when compared with neutron production by fission or spallation. This translates into economic advantages on target disposal, shielding requirements etc.

This report, written by leaders in lasers, laser plasmas, neutron sources, and neutron instrumentation & characterization, strives to describe the state-of-the art on such a laser-driven neutron source. We discuss the benefits of such a source for the applications that are possible presently at the LANSCE accelerator facility and beyond, ranging from materials science to solid state and nuclear physics. We also address technological issues still to be addressed as well as a brief discussion of other applications.

The first deployment of an in-house synchrotron in 2015 to Technical University München, Germany, illustrates how lasers transform another field hitherto constrained to large-scale user facilities [TUM 2015]. In this case, a laser replaces the undulator and allows to shrink the storage ring from hundreds of meters to less than five meters with a similar scale of reduction in investment cost. The unit is commercially available from Lyncean Technologies, Inc., Fremont, CA [Lyncean 2016]. The laser-driven neutron sources described here are at an earlier stage of their technical maturity, but similarly dramatic developments are expected.

For DOE/NE relevant programs, neutrons are a proven tool of great value for many applications in the field [Vogel 2013], and the development of compact, intense laser-driven neutron sources is relevant to these programs as follows:

- Laser-driven pulsed neutron sources open a path towards on-site or even pool-side characterization of fresh and in particular irradiated fuels for the Advanced Test Reactor.
- For future projects, such as new test reactors, laser-driven pulsed neutron sources provide the unique characterization capabilities offered by pulsed neutrons as outlined below at economically feasible extra cost, thus adding significant value in accelerating development and licensing of new fuel forms.
- Compact, reliable, and low-cost laser-driven pulsed neutron sources may also be utilized for in-line diagnostics such as measuring enrichment levels in fuel feed line for a molten salt reactor.

Building on the report by D. Chichester on alternative neutron sources for DOE/NE relevant applications [Chichester 2009], we summarize these exciting new capabilities in this report. For DOE/NE programs, the ability to deploy excellent characterization tools to irradiation facilities will mitigate the costly shipping of highly radioactive materials to LANSCE for advanced characterization. The LANL based DOE/NE funded Advanced Non-destructive Evaluation and Advanced Post-irradiation Examination program consists of three pillars, illustrated below. These are

1. Developing pulsed neutron based techniques to provide advanced characterization for novel fuel forms
2. Demonstrating and applying these techniques for ongoing efforts such as development of accident tolerant fuels and transmutation fuels.
3. Participating in advancing laser-driven pulsed neutron sources towards application, in particular for pool-side characterization at Advanced Test Reactor (ATR) at INL.

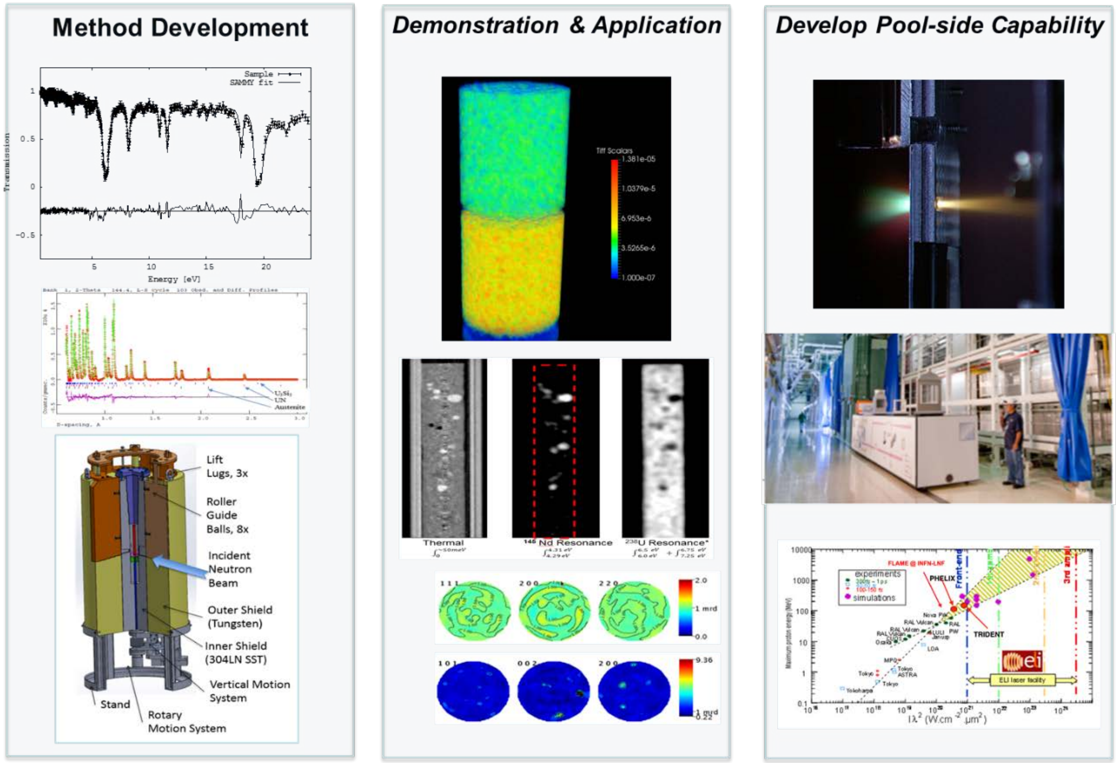

Figure 1: Three pillars of the LANL Advanced Non-destructive Evaluation and Advanced Post-irradiation Examination program.

2. Present neutron use and need for small & medium scale facilities

Neutron science is a wide field of research and development. The amount of possible applications is too extensive to be discussed in detail in this paper. Therefore, we will pick a few applications among those where we believe the proposed laser-driven neutron source might be a new asset to the field and which can be realized in the near future.

In nuclear physics, material science, biology, and related sciences, neutrons have been used to modify and diagnose matter. Because of their unique properties, they are a useful tool to explore areas where other diagnostics fail. Moreover, with their fundamentally different interactions with matter compared to charged particles or gamma rays, they are perfect for complementing established measurements and applications. In addition, neutrons produced either by spallation or nuclear reactions (i.e. giant resonance excitation) can serve to mimic reactions usually found in nuclear reactors and therefore help gain a better understanding of aging and stability of present and future nuclear systems.

As specified, there is a growing need for neutron sources of small to medium power, i.e. brightness comparable to older user facilities such as IPNS or LANSCE, with investment cost of on the order of a few tens of millions of dollars and physical dimensions to fit into a large room, i.e. not requiring large dedicated buildings. To review the state of the art and to underpin the need for those new sources we hereby quote the 2005 IAEA report on the *Development opportunities for small scale and medium scale accelerator driven neutron sources [IAE04]*:

Foreword: „[...] Small and medium power spallation sources will become more important as many small neutron producing research reactors are being phased out. [...] In addition to basic research theses alternate neutron sources will be important for educational and training purposes. [...] Neutron *applications in life sciences will be a rapidly growing research area in the near future. Neutrons can provide unique information on the reaction dynamics of complex biomolecular systems, complementing other analytical techniques such as microscopy, X rays and NMR. There is a general belief in the life sciences community that neutron methods are an emerging technique and not exploited to their full capacity. This is partly due to the fact that useful neutron beams can only be generated at advanced research* reactors and/or high energy neutron spa*llation sources.“*

The IAEA report focuses on small and medium sized particle accelerators and reactors which have been used to provide neutrons of high fluxes. Nevertheless, such a scheme is far away from flexible and there are many challenges to face. On the other hand, the underlying arguments of the IAEA report hold true for laser-driven neutron sources as well, as there is a growing need for flexible, high brightness sources that can be utilized at smaller laboratories. These boundary conditions can only be fulfilled by a laser-accelerated ultra-fast particle source.

As one application in mind, neutron resonance spectroscopy as well **as** radiography offers complementary information to X-ray diagnostics, especially because of the largely different cross sections for varying Z-materials. It therefore can serve as a novel diagnostic, for example to characterize spatial distributions of enrichment levels or fission product in ceramic fuels or characterize inclusions in metallic fuels.

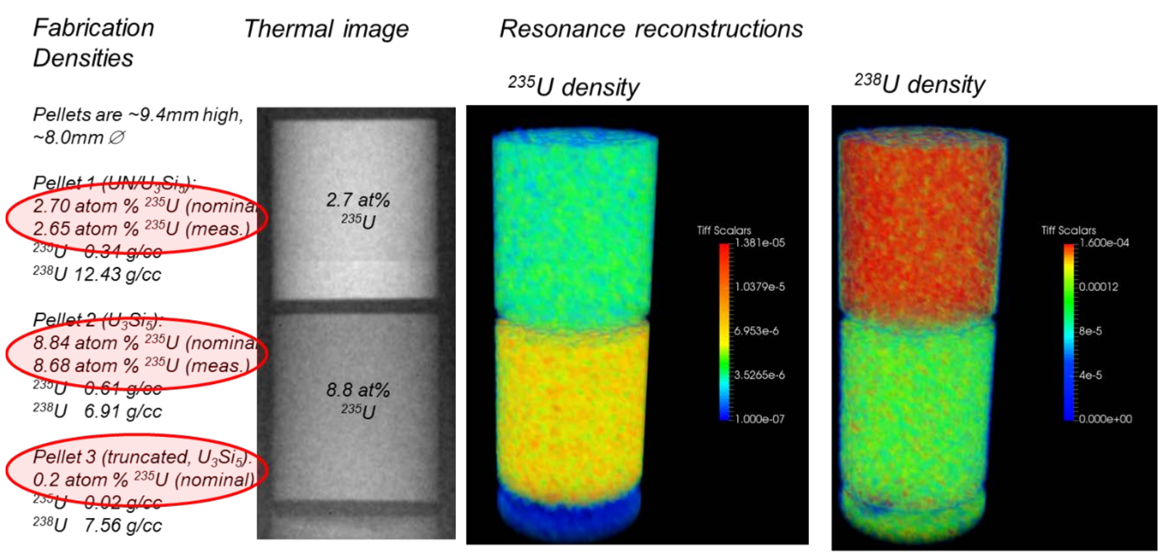

Figure 2: Characterization of three ceramic fuel pellets with different enrichment levels using computer tomography reconstruction of isotope specific densities. The agreement of nominal and measured enrichment is within ~0.1%.

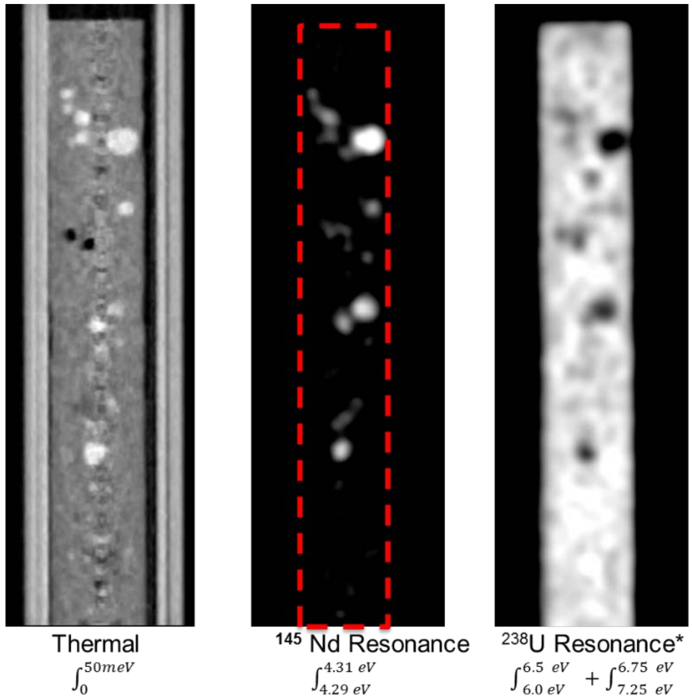

Figure 3: Characterization of a U-10 wt%Zr transmutation fuel with 5 wt% rare earth element inclusions. The thermal CT allows to measure gaps between the inner and outer container as well as fuel and container. However, inclusions are only visible as inhomogeneities whereas the ability to visualize locations of ^{145}Nd and ^{238}U atoms allows to unambiguously identify them as rare earth agglomerates [Vogel 2016a].

Ultra-intense lasers have been developed to a point where laser-driven particle sources, especially pulsed, intense deuteron sources, could potentially serve as a bright, compact neutron source. This would allow to bring the advanced characterization techniques developed at LANSCE to e.g. the Advanced Test Reactor at INL.

3. State of the art

This section describes the state of the art in lasers and conventional neutron sources to set the base-line for the description of laser-driven neutron sources.

3.1 Lasers

Since the invention of the laser [Maiman 1960], researchers have been on the quest for higher intensities to explore new phenomena. Pulsed laser systems in the nanosecond regime steadily increased from 1-TW to 100-TW over the two decades from the mid-70's to mid-90's, primarily by a succession of increasing high-energy and large-scale fusion-class lasers. The situation changed in the mid 1980's by the invention of the Chirped Pulse Amplification (CPA) scheme [Mourou 1985], that allowed pulses with significantly shorter final pulse durations to be safely amplified to high energies before recompression. This allowed TW-class lasers to down-scale from building-size to room-size, but also allowed high energy fusion laser technology to leap to the PW peak power level [Perry 1999]. Using such powerful systems, both room-scale femtosecond and larger picosecond lasers produced intensities of upto 10^{22} W/cm^2 an enabled researchers to explore relativistic laser/matter interaction (10^{18} W/cm^2), where electrons are accelerated close to the speed of light and the emission is strongly forward peaked due to the strong ponderomotive force of the light pressure [Wilks 1992]. Figure 4 shows the history of high power lasers.

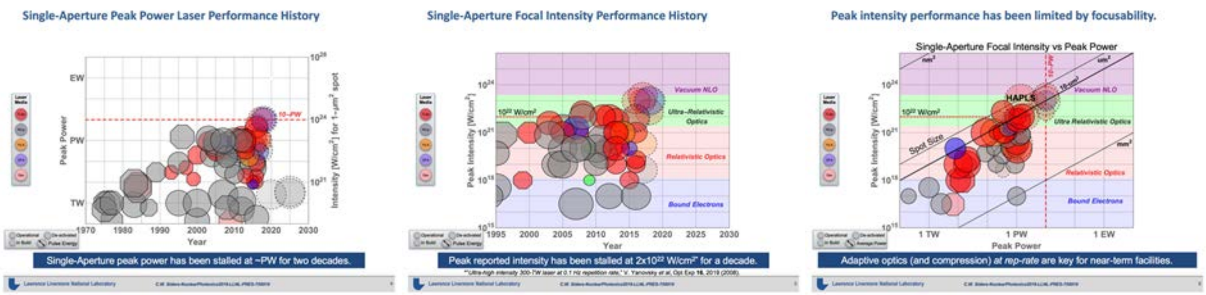

Figure 4: History of high power lasers. Left: Peak power versus year. The large jump in peak power in the late 1990's was achieved by the Livermore Petawatt Laser and over the next decade and a half duplicated by dozens of facilities globally. The late 2010's anticipate a second leap in peak power with the commissioning of several 10-PW class lasers currently under construction. Center: Peak focal intensity (reported) versus year, showing a similarly punctuated equilibrium evolution in peak intensity. Interestingly, during the 15-year „PW Plateau", peak reported intensities increased as rep-rate and active wavefront control improved the focusability of PW peak powers (right). The late 2010's will also show the commissioning of high rep-rate (10-Hz in the case of the HAPLS system) PW lasers, which are anticipated to achieve true diffraction limited intensities of 10^{23} W/cm^2 which have eluded PW system builders for two decades. Figures used with permission from C.W. Siders and C. Haefner, Nuclear Photonics 2016, Monterey CA.

In the late 1990's at LLNL, for the first time intense ion beams were observed originating from the irradiation of thin solid foils at the NOVA PW laser [Snavely 2000, Wilks 2001]. Since, laser driven ion acceleration has become a vibrant field of science around the world, leading to numerous publications and the discovery of heavy ion acceleration [Hegelich 2002], prompt- isochoric heating of materials [Roth 2001, Patel 2003, Roth 2008, Fernandez 2014], medical applications [Salamin 2008, Tajima 2008, Doria 2012], injector into conventional accelerators [Busold 2014], isotope production [Ledingham 2004, Kimura 2011] and novel diagnostic methods [Roth 2011]. Part of the huge international interest was the imminent prospect for applications as a powerful and very compact source many orders of magnitude smaller than conventional accelerator technology would allow.

Consequently, first experiments have started already in 2002 to use laser-driven ion beams to generate intense bursts of neutrons [Roth 2002], but the initial numbers were so far prohibitive from applications and the usage as a replacement for large scale facilities. Laser driven neutron production will be explained in more detail in the next chapter.

While PW lasers have become almost routine at various facilities around the world (see e.g. the overview by Danson et al [Danson 2015]), at present the next generation of high power short pulse laser systems are under construction in Europe (ELI [ELI 2011], Apollon [Papadopoulos 2016], SIOM 10PW [Gan 2017], and Korea [Sung 2016]. Those lasers, exceeding 10 PW peak power and foreseen to reach intensities of more than 10^{23} W/cm^2 will allow for higher ion energies and higher beam intensities in the coming years. It is worth nothing that besides peak power, also vast operation experience for a broad spectrum of laser facility exists, translating into reliability of laser systems.

Finally, the average power of ultra-intense lasers is rapidly increasing – presently the HAPLS laser, a 10-Hz 1-PW peak and 0.3-kW laser designed, built, and tested in LLNL and in process of transport to ELI-Beamlines in Prague for final commissioning, demonstrates a particularly effective gas-cooled multi-slab architecture which is scalable to perhaps 100-1000x higher average powers. For target geometries which are commensurate with the increased rep-rates, this would provide 100-1000x higher average flux of secondary particles.

3.2 Neutron Sources

The development of effective thermal neutron flux from the discovery of the neutron to the present day is shown in Figure 5 (left). After initial rapid increases, reactor-based neutron sources reached a maximum due to reactor safety considerations with the ILL in Grenoble, France, and HFIR at ORNL, U.S., facilities. Since then, all large-scale neutron research facilities were proton accelerator based spallation neutron sources such as SNS at ORNL, J-PARC in Japan, or the ESS in Lund, Sweden. However, the increment in thermal neutron flux is slowing down also due to considerations such as target heating as well as investment and operational cost of the accelerator.

Due to increased shielding demands for higher power neutron facilities, the closest sample positions may also increase, e.g. from ~6 m at LANSCE to ~15 m at SNS. The decrease in neutron flux on sample, following $1/L^2$, can only partially be compensated by neutron guides, which are only effective for cold neutrons, and in many cases frame overlap choppers have to be used to produce an optimized neutron energy spectrum at the sample position, further reducing the number of neutrons actually delivered to the sample and thus the gain for the experimenter from more powerful neutron source. The European Spallation Source ESS achieves an increase in thermal neutron flux by producing neutron pulses of 3ms in duration, compared to the e.g. 270 ns at LANSCE or 750 ns at SNS. While these longer pulses provide increased neutron flux for e.g. small angle scattering, vibrational spectroscopy, or reflectometry, other applications such as diffraction or energy-resolved neutron imaging require reduction of the flux by choppers to provide useful neutron pulses, essentially wasting some of the gains by the increase neutron output. Important parameters for the subsequent discussion are therefore the thermal neutron output, the closest possible distance to the source, and the neutron pulse width. It is worth noting that the 10^{10} n/pulse demonstrated by laser-driven neutron production at Trident are close to the first neutron spallation source ZING-P. Given the aforementioned advantages of laser-driven neutron production, a similar pace of laser-driven neutron sources as was observed for spallation neutron sources can be expected.

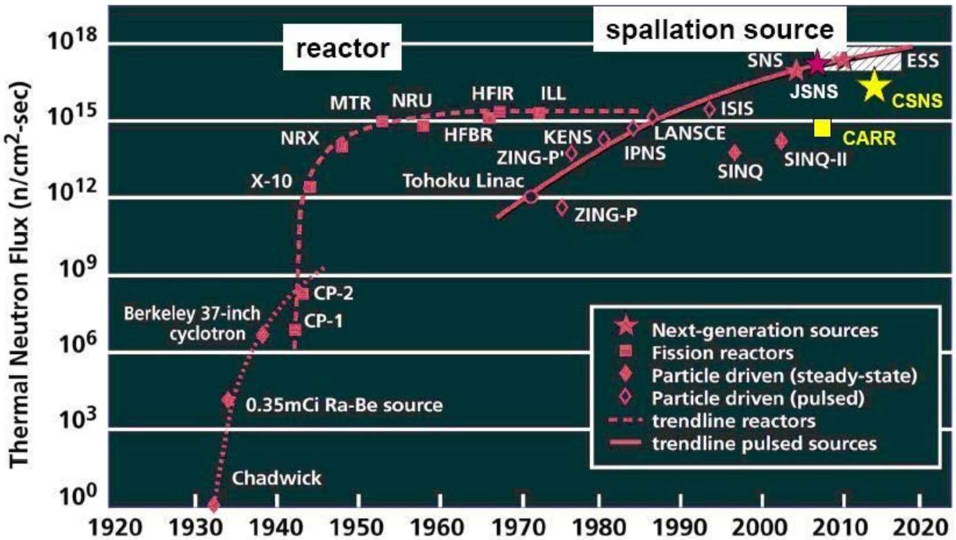

z

Figure 5: Historic development of thermal neutron flux [CSNS 2017] for comparison with the laser intensity evolution in Figure 4, center, and evolution of laser-driven neutron production in Figure 15. The 10^{10} n/pulse achieved at Trident place the development of laser-driven neutron sources approximately at the first spallation neutron source ZING-P (with the considerations about number of neutrons reaching a moderator described in the text).

Figure 5, right, shows the historic evolution of laser power for comparison. It can be stated that if neutron output for a laser-driven neutron source is at least linear with the laser power and this "Moore's law" continues for laser sources, laser-driven neutron sources may in the future allow for neutron sources that are not only less cost-intensive, but also provide more neutron flux than even the highest flux source planned or under construction at present. Furthermore, with the ~1 ns long pulses, the full flux may be used as no pulse shaping choppers are required (such as at the ESS, tacitly implying that the flux on sample is not benefitting from the increase overall neutron production) and with the reduced shielding demands of such a source, further increases in flux on sample are possible with a shorter source to sample distance, e.g. for imaging applications or bulk determination of isotope concentrations.

The more than seven decades of research with neutrons provides a vast experience with and tools for the design of the neutronics of target and moderators [Watanabe 2003], as well as with neutron instrumentation [Windsor 1981], captured in numerous text books and reviews. This promises a very rapid transition from initial development of production laser-driven neutron sources to productive deployment for the application.

4. Laser driven particle accelerators

Ultra-intense lasers have demonstrated the capability of accelerating short pulses of intense ion beams [Snavely 2000, Borghesi 2006]. These ion beams have been used to generate short bursts of neutrons by irradiating a converter in close proximity to the source, making this scheme a very compact and bright source of neutrons of up to more than 100 MeV in neutron energy [Roth 2013]. Using novel laser ion acceleration mechanisms, directed pulses of neutrons can be generated, which increases the brightness of these sources compared to previous attempts, but also compared to conventional neutron sources which produce neutrons with an isotropic distribution of trajectories, resulting in only a fraction of neutrons reaching the moderator and becoming ultimately available at the sample position. We review the recent research and present experimental data using a mechanism based on relativistic transparency to drive the most intense laser driven neutron source and use them for first applications.

Neutrons in general can be released from nuclei using energetic radiation. Electromagnetic radiation can excite collective modes that lead to neutron evaporation. Impact by energetic electrons or ions can release neutrons from the target nucleus or a high velocity ion can break up in the Coulomb field of another atom releasing one or more neutrons. In addition, neutrons can be released as a consequence of fusion reactions, as with present inertial confinement fusion experiments or using high-energy proton beams for spallation of heavy target nuclei. The promise of future ultra-intense lasers as drivers for brilliant, compact and highly efficient particle accelerators for electrons and ions, (potentially replacing in some cases much larger conventional accelerators) also ushers prospects for driving next generation neutron sources. While lasers at present cannot yet compete with accelerators or high flux reactors in terms of average power or neutron flux for medium size neutron sources as well as for high peak brightness neutron sources, they can complement large-scale facilities as powerful otherwise unavailable characterization tools and be easily attached to secondary drivers.

In the following we do not address the production of neutrons by thermonuclear fusion reactions, as this usually requires MJ laser systems the size of a football stadium. [Hurricane 2014]. Instead we will focus on neutron production using compact, high power short pulse lasers.

4.1 Photon induced reactions

Early experiments used excitation of giant resonances in nuclei to determine laser on-target intensities [Cowan 2000, Guenther 2012]. This research was motivated by the ultimate question “How much laser intensity actually reached the critical target surface?”. The interaction of the laser is driving a hot electron component into the target due to the ponderomotive force. The hot electron energy distribution function can be estimated according to Wilks [Wilks 1992] to scale with the laser strength parameter

$$a_0 = \frac{eE}{m_e \omega_L c}$$

(where e and m_e is the charge and mass of the electron, E is the electric field of the laser of frequency ω_L and c is the speed of light) resulting in a temperature equivalent to

$$K_B T_h = m_e c^2 \left((1 + a_0^2)^{1/2} - 1 \right)$$

The laser strength parameter is linked to the laser intensity by $a_0 \cong 0.85 \times 10^{-9} \lambda[\mu m](I[W/cm^2])^{1/2}$ and becomes of order of one at high intensities around $10^{18} W/cm^2$.

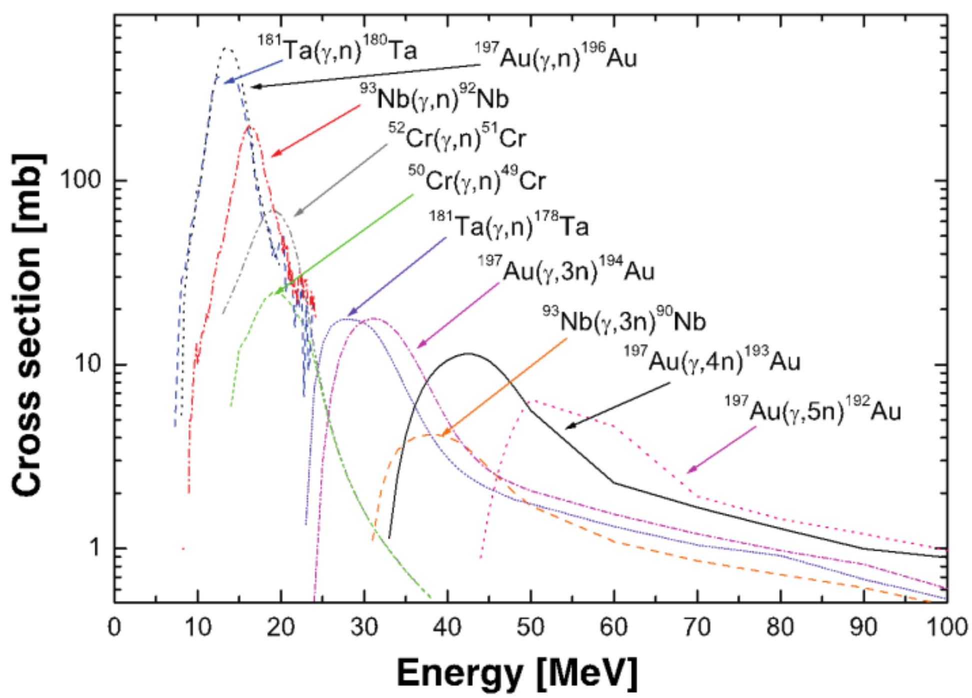

Figure 6: Energy dependent cross section for photonuclear (γ,xn) reactions for different isotopes (from [Guenther 2011]).

The Bremsstrahlung photons from this high-energy (i.e. hot) electron component therefore directly scales with the laser intensity with the higher the intensity, the hotter the electron component. The range of the Bremsstrahlung spectrum thereby can exceed the threshold of photon-induced nuclear reactions. Diagnostics based on photo-neutron disintegration reactions have been used to determine the laser intensity and reactions up to (γ,7n) in gold have been observed indicating the presence of 'hard' phwotons above 60 MeV [Cowan 2000] as can be seen Figure 6.

Recently photo-induced neutrons have gained new attention as new short pulse lasers have produced very short neutron bursts using low density targets in a pitcher-catcher geometry [Pomerantz 2014].

4.2 Cluster fusion

In the late 1990's the production of neutrons from short pulse lasers reached a new level using cluster targets. The interaction of a short, intense laser pulse with deuteron clusters of an optimum size of around 50 µm resulted in cluster Coulomb explosion and the subsequent generation of d-d fusion neutrons from a compact source. In the early experiments in 1999 around 10^5 n per shot have been produced [Ditmire 1999]. This method has been improved to result in a yield of 10^7 n/shot at the Texas Petawatt Laser [Bang 2013] that can deliver 120 J in a 170fs pulse. The source size in these experiments is of order only a few tens of microns (which is the focal region in the cluster volume) resulting in a high local flux.

5. Laser-driven ion acceleration

Laser particle acceleration is an important part of today's high energy and laser physics research. This young field of research has been opened by the advent of the *chirped pulse amplification* (CPA) [Mourou 1985], which allows laser peak powers up to the petawatt level [Perry 1999]. Today's laser facilities are able to investigate relativistic laser-matter interaction, or laser-plasma interaction, which is the basis for efficient particle acceleration with lasers. Laser-ion acceleration is primarily driven by relativistic electrons, generated by the interaction of an ultra-intense laser beam with a solid target or a gas jet. The laser peak intensity thereby has to exceed 10^{18} W/cm^2 to immediately accelerate electrons close to the speed of light. Today's lasers are able to reach maximum intensities of more than $10^{21} W/cm^2$ [Bahk 2004]. The dominant ion acceleration starts off the rear, non-irradiated surface by a rapid charge separation. This mechanism is known as *Target Normal Sheath Acceleration* [Wilks 2001] and has been investigated for about a decade. We briefly explain the mechanism before we will refer to new mechanisms.

Direct acceleration of ions would be possible with a laser pulse electric field strength of 10^{15} V/m at a given laser pulse intensity of more than 10^{24} W/cm^2. Those laser parameters are out of reach today and even in the future it would require extremely expensive facilities, thereby prohibiting applications like, e.g. medical and material irradiation facilities. Given the limits of present laser systems, the ion acceleration today is realized by the mechanism of charge separation.

5.1 Target Normal Sheath Acceleration

If a high intensity laser beam impinges on a solid target, already the rising edge of the pulse creates a plasma at the front side of the target. This effect is more dominant in the presence of pre-pulses or laser light originating from Amplified Spontaneous Emission (ASE). The interaction of the main pulse with plasma at intensities exceeding 10^{18} W/cm^2 accelerates copious amounts (more than 10^{14} and up to 50% of the laser energy) of free electrons in the laser forward direction, due to the ponderomotive potential of the laser beam [Boot 1957]. Other sources of relativistic electrons may also be present [Tajima 1979, Brunel 1987] but are of less importance for the acceleration.

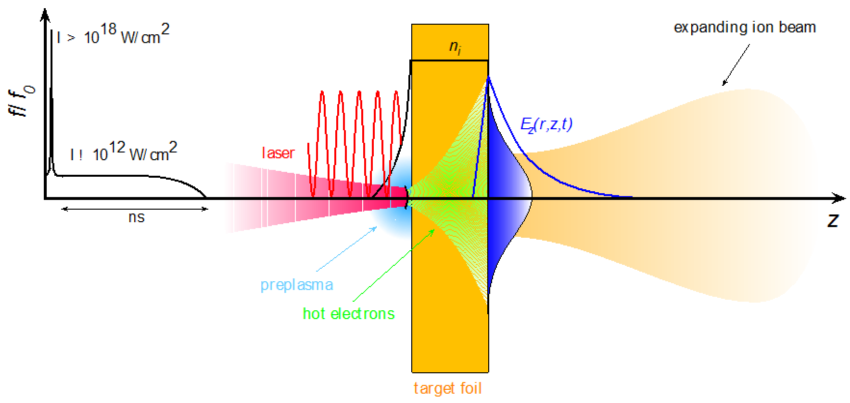

Figure 7: Target Normal Sheath Acceleration – TNSA. A thin target foil with the thickness d=5-50 µm is irradiated by an intense laser pulse. The laser pre-pulse creates a pre-plasma on the target's front side. The main pulse interacts with the plasma and accelerates MeV-energy electrons mainly in the forward direction. The electrons propagate through the target, where collisions with the background material can increase the divergence of the electron current. The electrons leave the target, resulting in a dense sheath. An electric field due to charge separation is created. The field is of the order of laser's electric field (TV/m), which ionizes atoms at the surface. The ions are then accelerated in this field, pointing in the target normal direction.

The electrons propagate through the solid target, escape from the target rear side (given an appropriate target thickness), and create a sheath field at the rear, undisturbed surface. The resulting field strength reaches several TV/m. Any surface atoms are thus immediately field ionized and accelerated off the target rear surface along the electric field lines caused by the electron sheath. Due to the thickness of the sheath of initially only a few micrometers, the acceleration of the ions is always normal to the rear surface, which leads to the name *Target Normal Sheath Acceleration* (TNSA) [Wilks 2001, Hatchett 2000]. Because of the screening of the field by the ionized atoms, only the ions at the surface are exposed to the maximum field strength and therefore are accelerated to the highest energies, whereas ions buried deeper inside the target are exposed to a reduced field strength and therefore accelerated to lower energies. Under usual experimental conditions the atoms at the surface stem from hydrocarbons, which naturally appear as contaminants. Among the available ions, protons have the highest charge-to-mass ratio off all ions, resulting in the highest kinetic energy during the acceleration.

An efficient ion acceleration by the TNSA mechanism requires an undisturbed rear surface in order to set-up a high field gradient. The generation of a pre-plasma by the laser pre-pulse or ASE can already produce a strong enough shock wave to disturb the rear surface and therefore influences the acceleration mechanism in the early stage. One crucial and important parameter for high intensity laser systems today is therefore given by the contrast of the system, described by the ratio of the precursory pedestrian of the laser-pulse to the main pulse. Most laser systems today operate at a contrast level around 10^{-6}, a few hundred picoseconds up to a few nanoseconds prior to the main pulse. Thus, a minimum target thickness is required to withstand the shock wave until the arrival of the main pulse.

Ions accelerated by the TNSA mechanism have an exponential energy distribution with an upper cut-off energy determined by the maximum of the accelerating electric potential. So far protons have been accelerated up to roughly 85 MeV [Wagner 2016] and heavier ions (Carbon) up to 5 MeV/u (MeV per nucleus) [Hegelich 2005], while it has to be noted that since the discovery of these ion beams in 1999 only limited progress has been made in terms of maximum particle energy. In addition to the high particle number and the excellent beam quality, e.g. small beam divergence [Cowan 2004] laser-accelerated ion beams have been proposed for a variety of applications, ranging from the ignition of a pre-compressed nuclear fuel pellet in inertial confinement fusion [Roth 2001] or the hadron-based radiation therapy in cancer treatment [Malka 2004].

5.2 Other Particle Acceleration Mechanisms

Access to energy ranges above ~100 MeV/u has been proposed by a set of new acceleration mechanisms, all based on ultra-intense laser-matter interaction. First, there is the so called *Radiation Pressure Acceleration* (RPA) [Robinson 2008], and second the *laser Break-Out Afterburner* (BOA) [Yin 2006, Yin 2007, Albright 2007].

The RPA mechanism is very demanding to the driving laser system. It requires focal spot intensities far exceeding $10^{22} W/cm^2$ and circular polarization of the laser light, which is beyond reach of today's laser systems. The BOA mechanism on the other hand only requires $10^{20}\ W/cm^2$ and linear polarization. Therefore, this mechanism has been tested already using present laser facilities having pulse length of 500 fs and energies of about 100 J on target.

The BOA mechanism has been discovered theoretically in 2006. The main difference between TNSA and BOA (or RPA) is the de-coupling of the ion acceleration from the driving laser field due to the thickness of the target in the case of TNSA (i.e. in TNSA ions are solely accelerated by the electrons removed from the target with the laser pulse, that may still be on-going, playing no role). In contrast, for the RPA and BOA mechanism the electrons that are accelerating the ions are still interacting with the laser field. In order to couple to the maximum number of available electrons, the target is required to be dense enough, such that the laser beam is not initially penetrating the target, but is coupling to the electrons. At some point the target has then to become relativistically transparent to the laser light, so that the light can directly interact with the electrons, co-moving with the ions at the rear surface. Therefore, the BOA mechanism starts as the above mentioned TNSA, but then during the raising edge of the laser pulse the intensity couples to the already moving electron-ion front at the rear side of the target. A theoretical description is given in [Yin 2007, Albright 2007]. In those publications the interaction of an ultra-intense short pulse laser was investigated using Particle In Cell (PIC) simulations for very thin solid targets, where the thickness matches only a few times the skin depth. After the initial phase, where the laser heats electrons, the product of critical density n_{cr} and Lorentz-factor γ equals the electron density of the solid, due to the mass increase of the swiftly oscillating electrons. The laser propagates through the target, continuously pushing the electrons, which transfer part of their kinetic energy to the ions. The energy loss of the electrons to the ions is then compensated by the presence of the light field until the total density drops due to the target expansion and the coupling becomes inefficient. Numerical simulations predict ion energies of hundreds of MeV for existing laser parameter and up to the GeV range for currently planned systems with the limitation towards experimental demonstration being the pulse-shaping possible at existing facilities. The required pulse shaping is of course under development at various laser facilities. The world-leading neutron production demonstrated at Trident, with an inferior laser power compared to other laser facilities, was the ability to shape the laser pulse much better than possible at more powerful laser facilities.

One important difference to TNSA is that in a mixture of target atoms which have reached the BOA regime, all of the accelerated ions propagate at the same particle velocity, governed by the slowest, i.e. the heaviest species present. Thus for high energy proton acceleration a pure hydrogen target is the ideal choice. For a given laser pulse duration and intensity as well as for each target composition one can determine an optimum target thickness, based on the above mentioned physics. High-Z target materials require, due to their larger number of electrons per atom, extremely thin targets in the realm of only a few nanometer thickness. This in turn requires laser contrast parameters which exceed the usually available values. For first systems the contrast has been demonstrated to exceed 10^{-10} using novel pulse cleaning techniques in the laser architecture [Shah 2009].

The experimental confirmation of the Break Out Afterburner (BOA) mechanism [Hegelich 2011, Jung 2013] lead to ion energies in excess of 100 MeV for the first time as well as the predicted change from a surface acceleration to the acceleration of the foil bulk material.

5.3 Neutron producing reactions

Due to the large cross section of neutron producing reactions, ions accelerated by conventional accelerators were widely used for neutron sources. The advent of laser-driven ion beams lead to the concept of compact ion beam-driven neutron sources. First experiments in 2000 resulted in $4x10^8$ n/shot using the 15 J laser pulses provided by the laser system at LULI ((Ecole Polytechnique, Palaiseau, France). In these first experiments, using a deuterated plastic target (the ‘pitcher’) and a titanium ‘catcher’ highly loaded with deuterons, the 2.45 MeV neutron signal from d-d- fusion reactions was clearly observed [Roth 2002].

During the following years, neutrons have been produced by laser-driven ion beams using the TNSA mechanism, which typically results in energetic proton beams as this mechanism preferentially accelerates surface contaminants according to their charge to mass ratio. First experiments explored the possible neutron yield for applications. The experiments did not address the applications directly but rather tried to optimize the neutron conversion efficiency in order to demonstrate the principle concept of laser-driven neutrons. In 2004, Lancaster et al used the $^7Li(p,n)^7Be$ reaction for fast neutron radiography applications [Lancaster 2004], in 2010 Higginson et al. increased the neutron yield to $2x10^9$ n/shot using the Titan laser at LLNL [Higginson 2010]. The result indicates the prospect for neutron resonance spectroscopy with laser-driven neutron sources. A year later, using short laser pulses of 360 J energy, the neutron yield was further increased and the maximum neutron energy was increased to 18 MeV [Higginson 2011]. This time not only was the yield increased to $8x10^9$ n/pulse but also a pronounced directed neutron emission had been observed. The basic reaction in all the above cases used the pitcher catcher configuration and the conversion of proton bunches into neutrons using light catcher elements (Li, Be) (see **Error! Reference source not found.**).

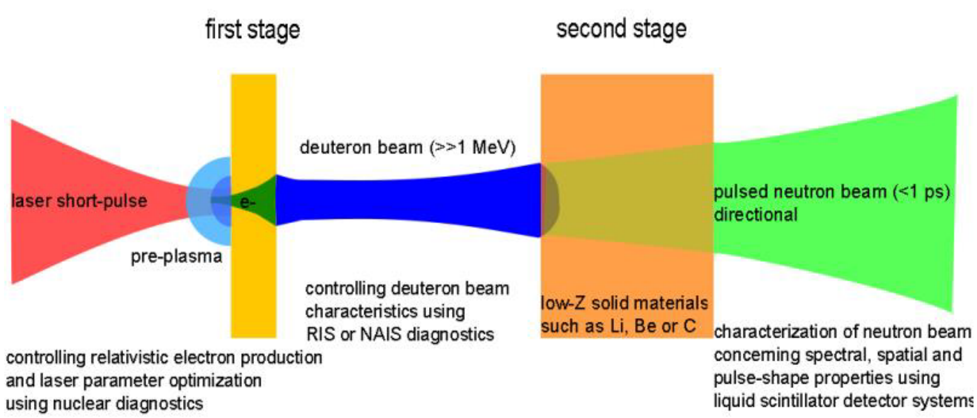

Figure 8: typical pitcher-catcher geometry for laser driven neutron production using ion beams.

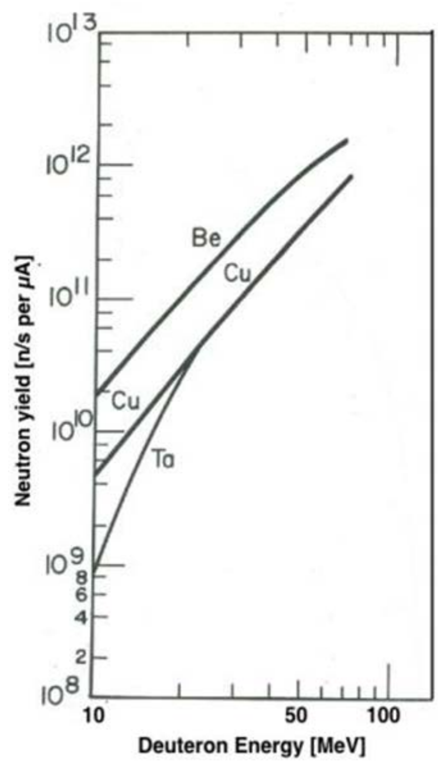

Figure 9: Neutron yield for deuteron induced reactions in an infinite catcher geometry (data from McMahan et al., Neutron beams from deuteron breakup at the 88-inch cyclotron, Int. Conf. on Nucl. Data for Science and Technology 2007)

The fundamental problem of the prior experiments was the limit in ion energy as the cross sections and therefore the yield for neutron production strongly increase with energy (see Figure 9 for deuterons). Moreover, to accelerate ions other than protons requires special target treatment or the controlled application of the ion species of interest as the rear side surface contaminant [Krygier 2015].

In recent years the contrast of high-energy short pulse laser pulses has largely improved allowing the irradiation of solid targets with thicknesses well below one micron [Wagner 2014]. At the same time the laser intensity at the target surface has increased to above 10^{20} W/cm^2.

[SV:] Acceleration of deuterons instead of protons allows utilizing the deuteron break-up reaction in which the loosely bound deuteron nucleus is separated into proton and neutron with either a proton stopped by the target nuclei and a neutron continuing to travel on the approximate trajectory of the deuteron or vice-versa (see below for a detailed discussion). Figure 9 shows the neutron yield for this reaction as a function of deuteron energy for Be, Cu, and Ta, indicating that Be is the most efficient target material. It is noteworthy that this type of data is based on very few measurement and only available for a few other target materials, indicating an opportunity for more research to identify optimal target material for deuteron break-up.

5.4 Neutron production

Ion beam-induced neutron production can be separated by ion kinetic energy: a high-energy regime with ion (mostly proton) energies from hundreds of MeV up to several GeV, and a low energy regime starting at a few MeV. For the high energy regime neutron spallation is favored by the use of heavy nuclei allowing for multiple, yet isotropic, neutron emission per ion impact. The advantage of multiple neutrons per incident particle comes at the cost of a several tens of cm beam range in the converter, with the correlated heat management issues, and initially high neutron energies. Furthermore, highly radioactive nuclei are produced in the target, leading to considerable shielding and decommissioning concerns. While resulting in a high total neutron number this regime is, at present, typically limited to very large accelerator facilities (e.g. the Los Alamos Neutron Science Center, LANSCE) [Lisowski 2006] and large converter installations. The low energy regime can be addressed with compact accelerators (e.g. cyclotrons) and most recently short pulse laser systems. For this regime low –Z converter materials offer the best ion to neutron conversion efficiency. While the number of neutrons produced is at most the number of particles reacting with the target, these systems generate forward directed distributions (vs. isotropic distributions in e.g. spallation or fission), which in turn allows to capture a much larger fraction of the produced neutrons in a moderator and thus use them more efficiently. Furthermore, these neutron production schemes offer significant operational advantages by much less demanding heating and absence of a significant radioactive inventory.

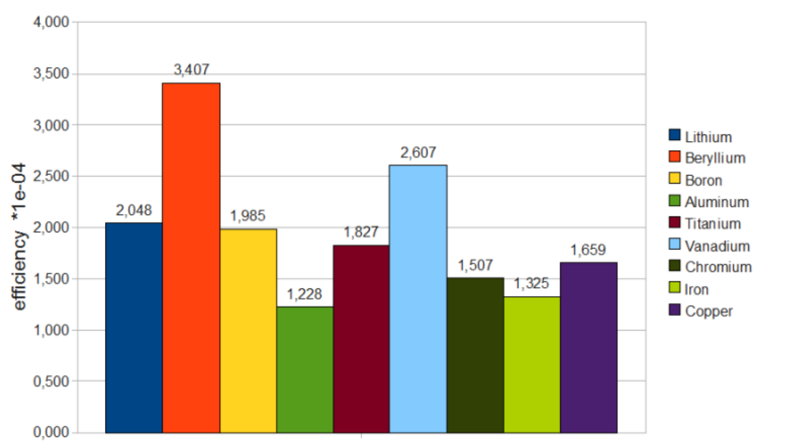

Figure 10: Simulated neutron production efficiencies per ion for different catcher isotopes assuming a typical, laser-driven ion energy spectrum (as observed with the Phelix laser). Simulations performed using GEANT4.

For the efficiency simulations in Figure 10 we have assumed a typical TNSA proton spectrum with a cutoff energy near 25 MeV (compare Figure 11). As efficient acceleration of the bulk material allows for the use of more efficient reaction channels for neutron production, the focus in laser-driven neutron production has changed from proton-induced reactions to deuteron-driven neutron production. The acceleration of deuterium offers two important advantages: First, every accelerated deuteron carries a neutron, which is loosely bound with a separation energy of only a few MeV and second, following separation, the remaining proton can still evaporate a further neutron on impact with the converter material. Assuming a purely Coulomb breakup, the deuteron with initial energy E_D decelerates as it approaches the target nucleus. At a certain distance from the target nucleus R_s the deuteron breaks up, with the proton and neutron each emerging with half of the initially available energy, E_D. On leaving the target nucleus, the proton gets re-accelerated in the Coulomb field [by repulsion of the nucleus] but the neutron keeps its given energy, E_n where $E_n = ½ (E_D – Ze^2/R_S – 2.22)$ MeV, (2.22 is the Q- Value of the reaction [Oppenheimer 1935]).

Figure 12 reveals distinction between p and d induced neutron reactions in light converter materials assuming an input spectrum that is typical for laser driven ion beams with a maximum cut-off energy near 25 MeV as can be seen in Figure 11.

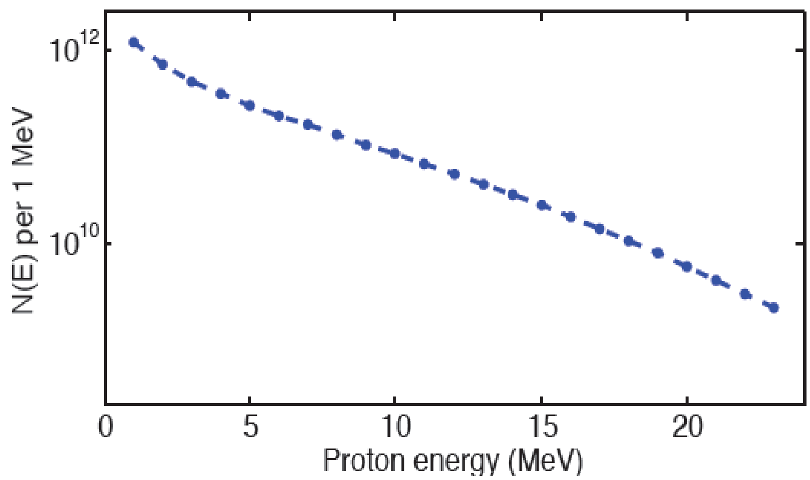

Figure 11: typical proton spectrum of an ultra-intense laser

As a further benefit, because neutrons from the deuteron breakup carry a large momentum in the direction of the incident particles, i.e. the initial laser pulse, the neutron's angular distribution becomes non-isotropic acquiring a distinct forward directionality. This results in higher neutron flux captured by a moderator or available neutrons for fast neutron methods as well as reduced shielding requirements compared to the isotropic spallation neutron sources. [SV:] Furthermore, the target thickness for e.g. Be targets is around 1 cm with a diameter of about the same being sufficient to capture the deuterons emitted from the laser target. This is an order of magnitude smaller than a spallation target (e.g. two stacks W disks of ~10 cm diameter and ~10 high at LANSCE's target 1 [Mocko 2013]). A typical moderator thickness to slow down spallation neutrons (up to 100 MeV initial energy) is 2.5 cm (e.g at LANSCE) [Ino 2004, Mocko 2013]. A somewhat thinner moderator is required for the lower neutron energies resulting from deuteron break-up of laser-accelerated deuterons. The combination of the two allows sizes of the neutron source, consisting of laser target, deuterium target, and moderator, of a few cm. Since much less shielding is required compared to a spallation neutron source, and laser beams can be transported in vacuum tubes of a few cm, this may eventually enable intense pulsed neutron sources e.g. in hot cells (with the high energy neutrons hitting a beam stop).

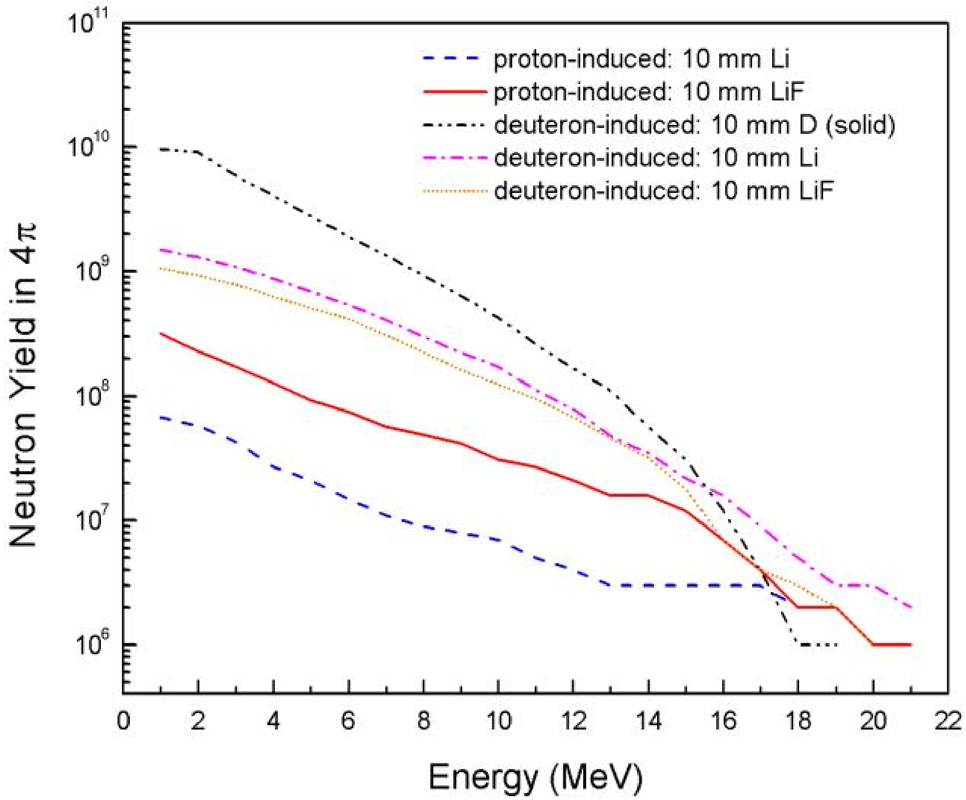

Figure 12: Energy-dependent proton and deuteron induced neutron production using 10^{13} ions from a typical laser source at a cutoff energy around 25 MeV/u. (like in Figure 11)

With the use of solid target foils of sub-micron thickness and high contrast laser systems, recently the neutron yield has increased by orders of magnitude compared to the TNSA based earlier attempts. In 2012 experiments at the Trident laser at Los Alamos National Laboratory resulted in a yield of 10^{10} n per laser pulse and a neutron energy in excess of 100 MeV using 80 J pulses of 600 fs duration incident on a 3µm diameter spot [Roth 2013, Jung 2013a]. The neutron distribution also revealed a clear directionality. This was accomplished using a thin, deuterated plastic target (pitcher) and a sealed Be catcher. In this work neutrons had been used for the first time to perform for static neutron single shot radiographs with fast neutrons. In 2013, the non-isotropic forward yield was further optimized with a cylindrical tungsten reflector around the Beryllium converter. In 2015 experiments at the Phelix laser system at the Helmholtzzentrum für Schwerionenforschung – GSI in Darmstadt [Neumayer 2005] lead to a neutron yield of 2x 10^{11} n/pulse with incident laser pulses of 80 J energy and 450 fs duration. In both cases the neutron flux was strongly peaked in the forward direction. The catcher material and geometry has been improved to match the several centimeters range of the ion beam. Consistent with the predictions from relativistic transparency, there was a strong dependence on the target thickness; targets that are too thin become transparent well before the maximum laser intensity and those that are too thick do not become transparent at all. In these extreme cases the expected lower energy ion beams generate an order of magnitude lower neutron yields from the catcher. The neutron pulse duration is basically determined by the time the ion beam needs to pass the catcher. Given the fact that the ion beam has an initial pulse duration of only a few ps and taking into account the temporal dispersion and pulse lengthening commensurate with the energy spread of the beam (i.e. ion debunching) the neutron pulse can be of sub-nanosecond or nanosecond duration. This novel short pulse capability enables various applications as described below.

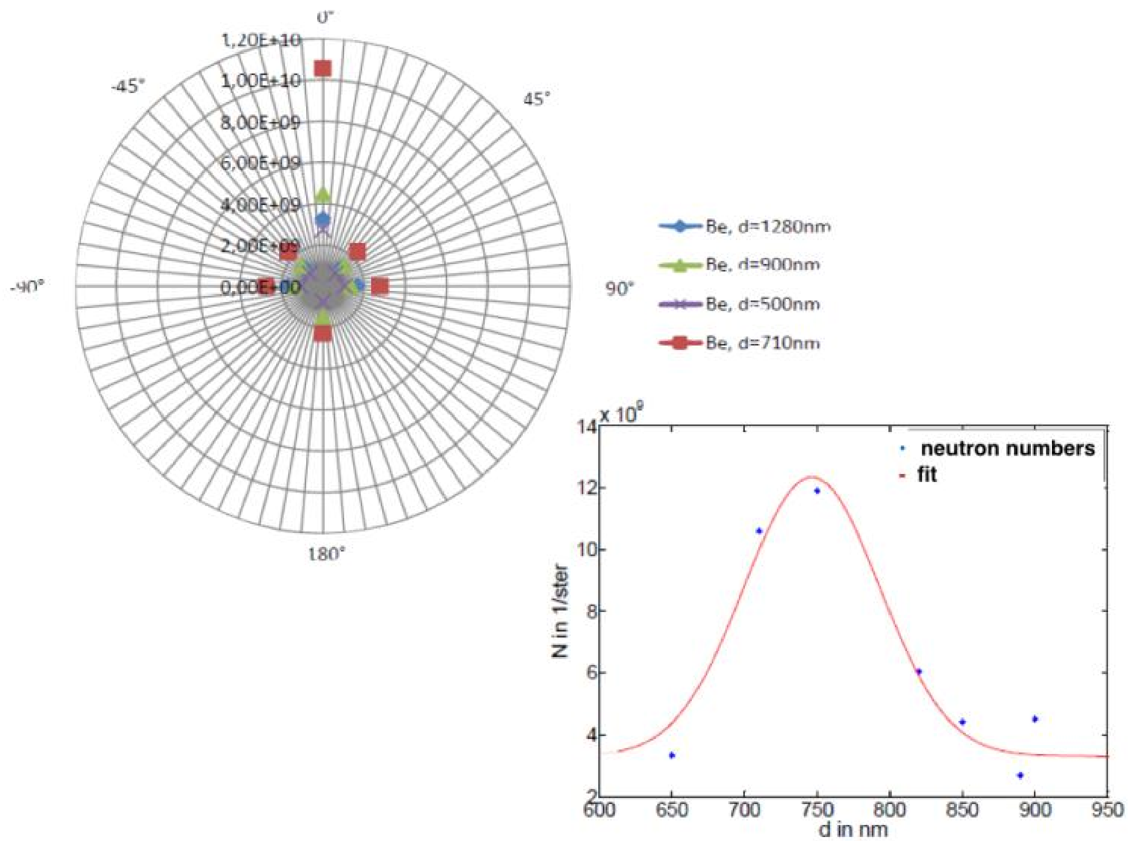

Figure 13 Target thickness sensitivity and directionality of the neutron emission based on ion beams accelerated in the relativistic transparency regime.

6. Prospects

Lasers have been used to produce neutrons for many decades, but with different approaches than the one described above. Apart from those experiments, aimed at pursuing thermonuclear fusion, it has become clear, that the development of modern short pulse lasers has been a breakthrough in this endeavor. First using cluster targets, then intense electron beams and after the discovery of laser-driven ion beams, the use of (p,n) reaction demonstrate that short-pulse lasers have become an ever more efficient tool to produce intense neutron pulses. With the enhancement of the laser contrast and the exploration of the relativistic transparency regime, laser driven sources now have entered a pulse yield level that is already suitable for real world applications so far limited to large scale user facilities. The recent jump in neutron numbers mark only the beginning of what laser-driven sources might be able to do in the near future. Higher laser pulse energy, paired with higher wall plug efficiency (due to diode pumping) and higher repetition-rate, each can add at least an order of magnitude to the average neutron flux. With costs on the order of $10M per laser, tens of synchronized lasers could be envisioned feeding a single moderator to devise a pulsed neutron source far surpassing existing spallation sources at equivalent investment cost (2-

3 billion dollars). On the other end of the application spectrum, laser-driven neutron sources with neutron output similar to the Intense Pulsed Neutron Source (IPNS) at Argonne National Laboratory can be envisioned. The IPNS was a workhorse neutron source for several decades and its capabilities could be deployed at facilities requiring powerful on-site characterization such as the ATR.

Just based on the current experimental findings, a 200 J / 20 Hz laser with high contrast should already provide around 2×10^{13} n/s. Utilizing the predominantly forward momentum, we conservatively estimate 1.5×10^{13} n/s are injected into the moderator. For comparison, at the LANSCE spallation source, a 100 μA 800 MeV proton current provides proton pulses for spallation at 20 Hz, corresponding to 3×10^{13} p/pulse and at a conversion of 20 n/p in spallation 6×10^{14} n/pulse. These neutrons are produced isotropically, with about 30% captured in one of the four thermal neutron moderators. A single moderator feeds the diffraction beam line HIPPO and the imaging beam line Flight Path 5, resulting in about 7% of the produced neutrons reaching the moderator for these two instruments. This results in about 2×10^{13} n/pulse or 4×10^{14} n/s (at 20 Hz) required in a moderator to achieve the performance of the two aforementioned instruments for which results were reported in several previous reports [Vogel 2015a&b, Vogel 2016a-c].

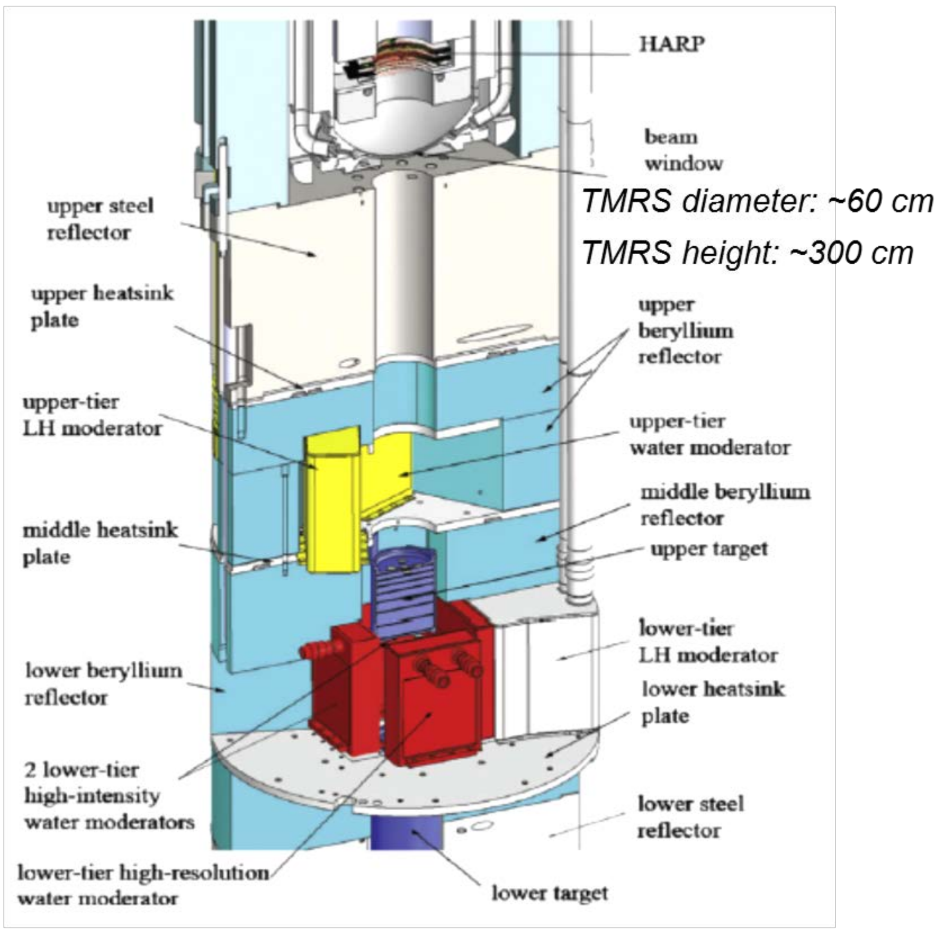

Figure 14: Schematic of the LANSCE target-moderator-reflector-shielding (TMRS) system. The water moderators are shown in red with the stack of tungsten disks shown in blue being the spallation target [Mocko 2013].

Considering that in the case of the laser-driven system using the deuteron break-up the majority of the forward traveling neutrons could be captured by a moderator, a 200 J/20 Hz laser-driven source - a device feasible today - would be only an order of magnitude lower in flux than LANSCE. At LANSCE, the closest moderator to sample/detector distance is ~6 m (with 9m used on HIPPO and between 8 to 11 m for the energy-resolved imaging). Due to the compact size of the laser-driven system, a moderator to sample/detector distance of ~2m is possible (1.25 m were demonstrated at Trident). With the flux decreasing with $1/L^2$, for some applications, such as low/medium resolution neutron time-of-flight diffraction or energy-resolved neutron imaging, such a laser-driven neutron source would be already equivalent to the LANSCE beamlines.

With the commissioning of the most modern systems, such as BELLA, ELI or Apollon [Zou 2015] for neutron experiments new research can be envisioned that makes use of the excellent beam properties. As can be seen in Figure 15, the yield of laser driven neutrons per pulse has been increasing over the last few years and with the upcoming facilities can close the gap to large scale spallation sources. Development of state-of-the-art lasers for these facilities will reduce the cost for smaller, less intense systems, making them more economic for smaller applications. Finally, as smaller systems can be fielded at universities laser-driven neutron sources can serve as a breeding ground for the next generation of young scientists in neutron science.

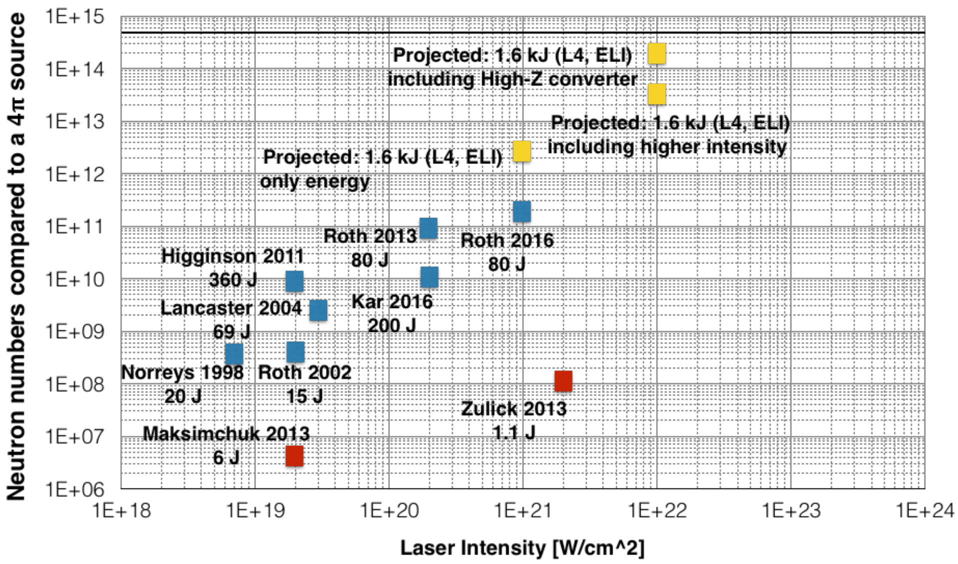

Figure 15: Number of neutrons per pulse from a laser driven neutron versus laser intensity. The neutron numbers of the directed neutron beam are compared to a conventional isotropic neutron source. Results in red indicate short pulse lasers below 100 fs, blue are high energy lasers around 0.5 ps pulse duration and the yellow marks indicate the prospect for upcoming systems currently under construction.

7. Novel Cryogenic Deuterium Jet Targets for Laser Neutron Sources

One of the authors of this report (S. Glenzer) participated in the development of a novel deuterium target design that may allow continuous operation of a laser-driven neutron source at 10 Hz [Kim 2016, Gauthier 2016, Fletcher 2016]. This design is described in detail in this section to illustrate that not only do pulsed lasers and pulsed neutron target/moderator systems exist, but also that technology to provide a continuous deuterium target is under development.

SLAC National Accelerator Laboratory and Stanford University have demonstrated advanced laser-ion sources and novel accelerator technologies to make urgently needed ion and deuteron beams available for research and applications. The design uses a cryogenic micro-jet that emanates from a nozzle with speed of 100 m/s to provide a replenishing target at laser focus. These targets have been operated with hydrogen, hydrogen/deuterium mixtures and pure deuterium. Experiments have produced

1. Small normalized emittance of 0.1 mm mrad,
2. High quality 20 MeV proton beam in the TNSA regime
3. 80 MeV proton beams in relativistic burn-through regime
4. Simultaneous proton and deuteron beams at equivalent same energy/nucleon
5. Pure deuteron beams

A target development is in place to continue developing these jets and optimize to the shape to access advanced ion acceleration physics mechanisms.

7.1 Cryogenic Laser proton source and deuteron acceleration system

Advances in the development of intense short pulse lasers have led to exciting progress in plasma-based ion acceleration. Production of energetic ion bunches from compact laser-plasma systems [Macchi 2013] have attracted great attention due to the wide range of potential applications, from injectors for conventional accelerators, to proton imaging and oncology.

The SLAC design is based on a novel cryogenic hydrogen micro-jets and Joule-class high-power laser systems. The ion source is produced by laser irradiation of a hydrogen jet target. The jet emanates from the nozzle with a speed of 100 m/s and is thus a suitable high-repetition rate source for protons and can deliver heavier hadrons, i.e., deuterons, carbon ions, or neon ions if needed.

Figure 16 shows the results from our 3-D particle in cell simulations. We observe that the principle laser acceleration mechanism is due to target normal sheath acceleration (TNSA). In addition, beneficial effects due to relativistic transparency start to set in for these conditions. The simulation results together with experimental evidence from our first proof-of-principle experiments show that we can achieve the following parameters: 10^{10} protons at (20 ± 1) MeV at a repetition rate of 1 Hz. These repetition rates are currently the state-of-the art and unsurpassed by alternative laser acceleration approaches. These simulations are a tool for optimization of the laser proton source and have successfully guided the development. They indicate that further optimizations of proton energy, emittance, and dose may be possible by the choice of laser wavelength, contrast and target thickness. Figure 16 also indicates benefits of relativistic transparency where a proton energy boost is observed when the laser burns through hydrogen and the laser beam interacts with protons on the backside of the target.

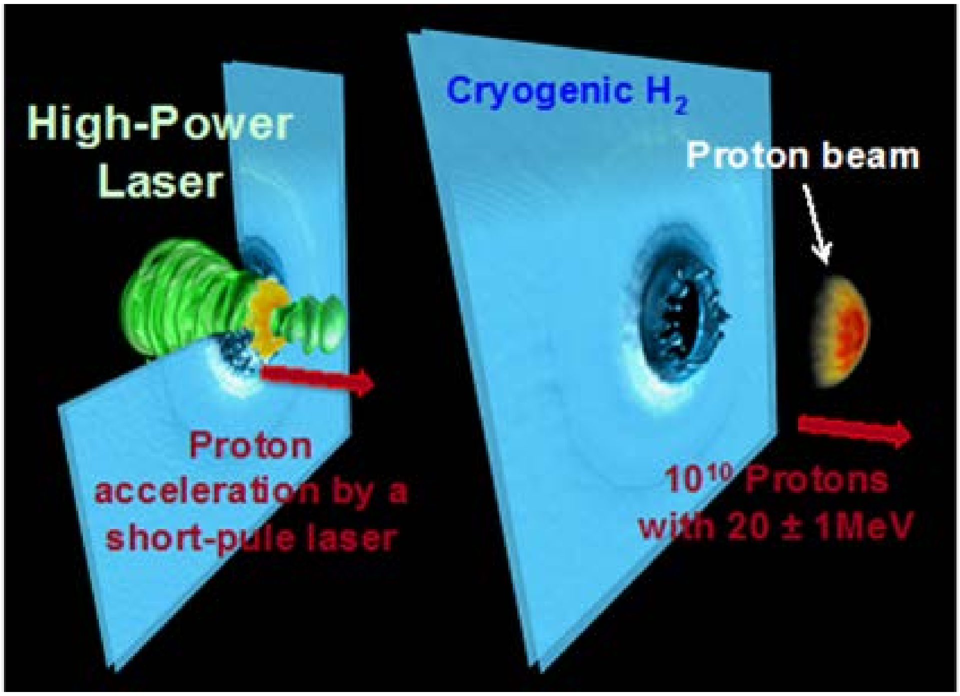

Figure 16: Results from 3-D particle in cell simulations using the code OSIRIS show the production of a high-energy proton pulse. These simulations indicate the hydrogen jet in blue, the laser in green, and protons in orange-red. At the end of the 50fs-long laser pulse, a pure energetic proton beam with 10^{10} particles emanates from the target. The proton beam energy of 20 MeV and its normalized emittance 0.1 mm-mrad meet requirements for injection and acceleration with a high-gradient rf accelerator.

Laser-interaction experiments with cryogenic hydrogen have been performed by Stanford researchers as part of a DOE-funded program to investigate the physical properties of dense hydrogen. These studies provided first-class data that show great promise for new research into the proton acceleration mechanisms suitable as a source for injection. Figure 17 shows the cryogenic hydrogen micro-jet implemented at SLAC National Accelerator Laboratory. A jet with 5 µm diameter is shown here, albeit smaller thickness micro-jets with 1 µm thickness have already been demonstrated at Stanford that initially show performance in line with that required for the proton source needed for oncology. The figure demonstrates the stability of the jet where the laser beam interaction with the jet has been measured with well-characterized density profile from interferometry and shadowgraphy data indicate a spatial stability of 1 µm rms.

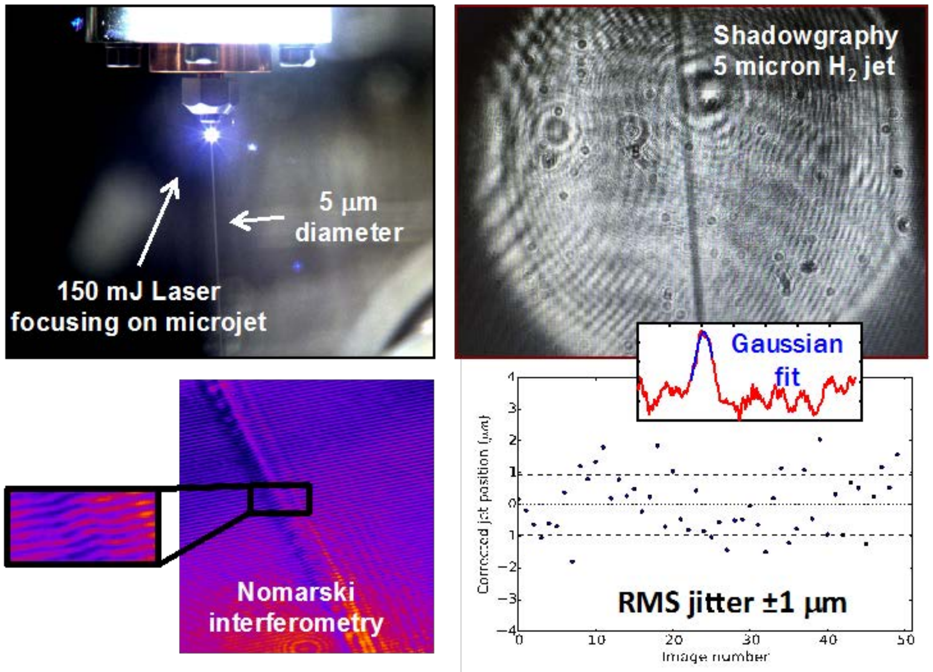

Figure 17: Stanford's continuously flowing cryogenic hydrogen micro-jet for laser-driven plasma acceleration experiments (LCLS experiment 2015). (Top left) Image of a 150 mJ, 45 fs laser beam interacting with the jet is shown. The laser was focused to a 4 µm laser focal spot hitting the target at 1 Hz. (Top right) The jet's spatial stability has been measured with shadowgraphy and the data shown on the bottom right indicate stability of 1 µm rms. (Bottom left) The jet density profile has been measured in situ with a probe laser using interferometry.

First proof-of-concept laser experiments with the jet have been performed at several user facilities: Matter in Extreme Conditions (MEC) instrument at the Linac Coherent Light Source, the DRACO laser at the Helmholz Zentrum Dresden Rossendorf (HZDR), the Titan laser at the Lawrence Livermore National Laboratory, and the Texas Peta Watt Laser facility. An experimental schematic for energetic deuterons is shown schematically in Figure 18 below.

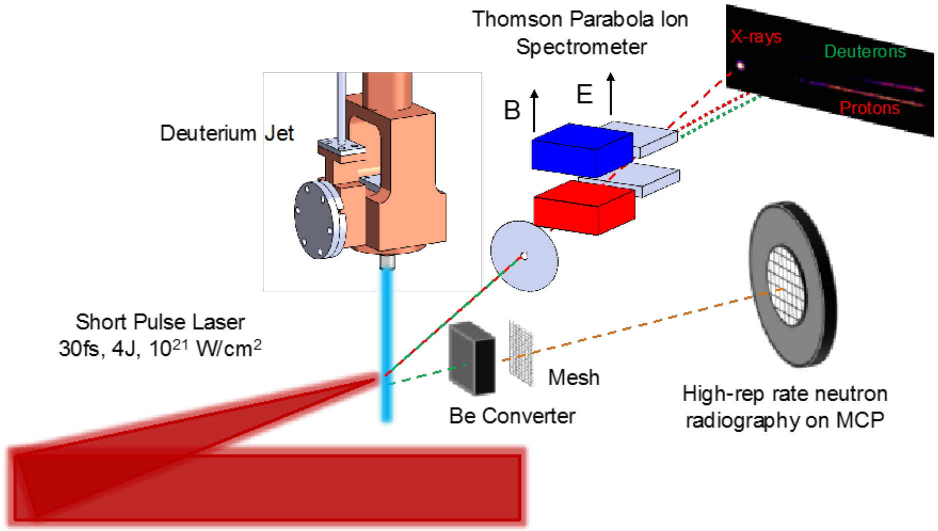

Figure 18: The experimental setup of a proton acceleration experiment using cryogenic micro-jets target is shown. A 4 J, 30 fs high-intensity laser pulse is focused on the micro-jet using a mixture of hydrogen and deuterium. The laser-driven proton and deuteron beam is investigated using a radiochromic film (RCF) stack, Thomson parabola spectrometers and Be converter with a multi-channel-plates (MCP) for neutron radiography. The Thomson parabola data are an example from an experiment at Titan.

In addition, experiments have been performed at the 200 TW Draco laser. The maximum proton energies in the first J-class laser experiments are about 10 MeV. The spectra indicate TNSA-like spectra with some additional spectral peaks. These proton beams can be generated at high repetition rates. Here, we demonstrate high-repetition rate laser-driven proton beams with a 100 TW laser system achieving high averaged flux. Figure 19 shows an example of data from a 60 second-long run at 1 Hz.

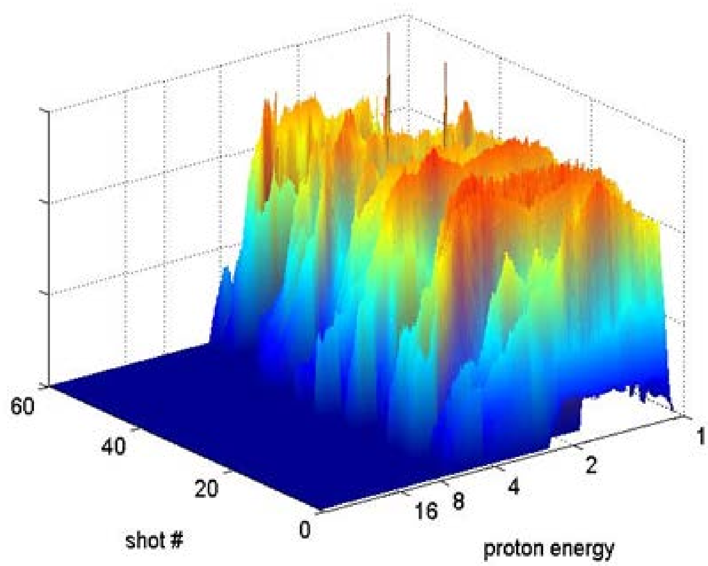

Figure 19: Proton spectra are shown from cryogenic hydrogen measured for 60 seconds and at 1 Hz. This target allows achieving high dose.

These results show that the proton energy is well reproduced from shot to shot and consistently peaking in the 5-8 MeV range. Recent studies (June 2016) have achieved 20 MeV proton energies by reducing the laser pre-pulse. The goal for the laser-proton source is to use simulation-experimental confirmation to design a high quality 10^{10} proton/shot source. This detail is described in the simulation section below.

7.2 Simulations

A series of 3D particle-in-cell (PIC) simulations to explore the acceleration of protons from this hydrogen targets with a 4 J 50 fs laser have been done using the state-of-the-art code OSIRIS [Fonseca 2002]. OSIRIS is a PIC code that models plasma as charged particles interacting self-consistently via the electromagnetic fields they themselves produce. These models work at the most fundamental, microscopic level, and thus can provide an accurate description of the plasma physics associated with the laser-plasma interaction and particle acceleration.

Target thickness is critical, and the transition from pure TNSA (5 μm targets) to a relativistic transparency enhanced TNSA (1 μm targets) regime can improve performance significantly. For example, initial results show that with a 5 μm thick target, maximum proton energies of 30 MeV (Figure 20), with ~2×10^9 protons at 20±1 MeV are realized. Protons are accelerated by the TNSA mechanism and their divergence angle at 20 MeV is ~ 6°. In order to optimize the proton energy and number, target thickness was varied from 0.5 – 10 μm where 1 μm was determined to be the acceleration optimum, reaching a maximum energy of 65 MeV and with ~10^{10} protons at 20±1 MeV (Figure 20).

This optimization is associated with the transition from TNSA in opaque targets to relativistic transparency acceleration. For thin targets, as the laser heats electrons the target starts expanding and the peak density drops. At some point during the interaction the density reaches a level where the target becomes relativistically transparent. This occurs because in the presence of an intense laser field electrons will oscillate with a Lorentz factor ~ a_0, where $a_0 = e\,A/m_e c^2$ is the normalized vector potential of the laser (e is the elementary charge, m_e is the electron mass, and c is the speed of light in vacuum). This will lower the critical density for laser propagation to n_c/a_0, where n_c is the non-relativistic critical density. The laser is then allowed to propagate through the target and interact with the hot electron cloud responsible for the proton acceleration on the rear side of the target. This replenishes and re-heats the electrons responsible for protons acceleration, thus leading to a more sustained TNSA electric field and to higher proton energies. We observe that in this regime the maximum proton energy is approximately twice the energy of the TNSA case.

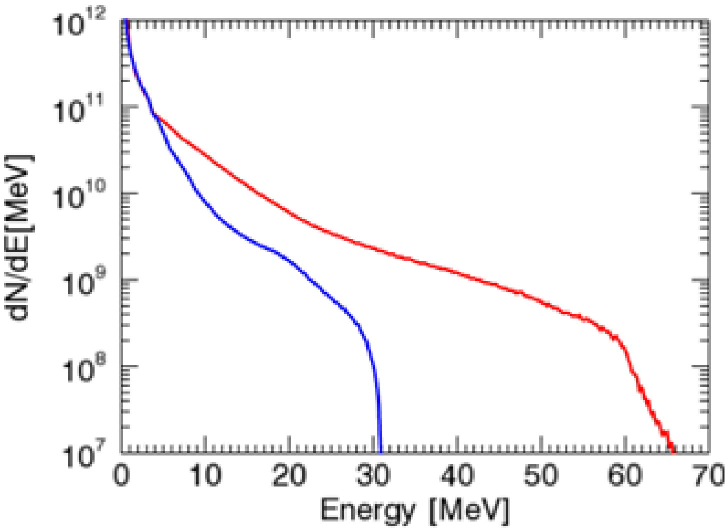

Figure 20: Proton spectra from the interaction of a 4 J, 50 fs, $8x10^{20}$ W/cm^2 laser with a hydrogen target with thickness of 1 μm (red) and 5 μm (blue). The number of protons with 20±1 MeV is ~ 10^{10} (red) and $2x10^9$ (blue).

8. A "Laser-LANSCE" Facility

To illustrate the potential and provide a quantitative assessment how far apart a laser-driven facility would be away today from the capabilities of the Los Alamos Neutron Science Center, we describe the LANSCE facility, discuss pros and cons of a similar laser-driven facility and how it would compare for operational parameters including investment and operation cost.

8.1 Overview of LANSCE

At the core of LANSCE is the 800 m long 800 MeV proton accelerator that drives various applications, making it unique when compared with accelerator facilities that only drive a thermal neutron sources. The LANSCE accelerator provides protons for the following applications:

- 100 MeV protons are used at a 250 μA proton current for target irradiation to produce medical isotopes.
- 800 MeV protons are used at a 100 μA proton current to produce cold, thermal and epi-thermal neutrons at the Lujan Center at 20 Hz. These neutrons are used for material science, solid state physics, and nuclear physics.
- 800 MeV protons are used to investigate the interaction of such beams with matter in the Blue Room, e.g. for spallation target development.
- 800 MeV protons are used to produce spallation neutrons which are delivered without moderation to the samples, providing neutron energies from 0.1 MeV to 600 MeV. These neutrons are used to measure interaction cross-sections as well as for testing of radiation hardened integrated circuits for aerospace applications.
- The 800 MeV protons are used to investigate dynamic phenomena, such as shock waves, with sub-microsecond time resolutions and penetrating centimeters of materials for sample and

containment vessels. Contrary to neutron and X-ray flash radiography, magnetic lenses allow magnification for proton radiography.

- Neutrons are slowed down to the ultra-cold energy regime to study fundamental properties of the neutron such as life time or electric dipole moment.

We will discuss key applications of each facility and show how a laser-driven pulsed neutron source could provide such capabilities at a much lower cost and even with operational benefits in some cases.

8.2 Thermal neutrons for material characterization

Thermal neutrons are used for microstructural characterization (texture, dislocation densities, phase composition) as well as stress/strain measurements. Pulsed thermal neutrons have the advantage that diffraction angles are constant and in principle pinhole-shaped incident beam path and diffracted beam path at e.g. 90° diffraction angle are sufficient to characterize a sample for these parameters. In particular for irradiated materials, pulsed neutrons allow the design of shielding containers with small openings, reducing exposure from the radioactive sample. At LANSCE, target 1 is the thermal neutron source. As described above, a laser-driven system based on laser systems existing today (e.g. 200J/20Hz) could compete with this facility. The very narrow pulse width (<1 ns compared with 270 ns at LANSCE) does not provide benefits for thermal neutrons since the moderation time determines the diffraction peak broadening and therefore the resolution. The second major contribution to the resolution is the flight path length L, measured from moderator to sample. If the HIPPO neutron diffractometer were to be operated at such a source, the count times would be about 10 times longer. Given that HIPPO can characterize a sample of ~0.5 cm^3 in <1 hour for phase composition and texture in most cases, this is still acceptable for operation and comparable to older sources (IPNS) or count times at reactor sources. For thermal neutron imaging and tomography, moving sample and detector closer to the source may still provide sufficient resolution to obtain e.g. pellet dimensions and identify voids and cracks, at similar count times as LANSCE's Flight Path 5, i.e. minutes. This would allow thermal neutron CT where the pulse structure of the neutron source can help to discriminate against gammas emitted from a highly radioactive sample. While a diffractometer such as HIPPO requires investment in excess of $1M, imaging capabilities with e.g. a large detector panel and several scintillator screens are available for <$100k.

8.3 Epithermal neutrons for material characterization and cross-section measurements

Moderated epithermal or thermal neutrons can be used to identify isotopes based on their characteristic energy-dependent absorption cross sections. In order to use laser or accelerator driven neutrons they have to be moderated, i.e. slowed down. Sub-nanosecond neutron pulses, providing only a negligible contribution to the energy resolution from the initial pulse for resonances up to ~10 keV, and a compact moderator system allow for high quality neutron spectroscopy [Pomerantz 2014]. While the recently demonstrated LANSCE proton pulse width reduction from 270 ns to 30 ns was only observable for resonances above ~5 keV (while most resonances used for NRTA are below 100 eV), pre-moderation pulse-width of less than 1 microsecond are required to perform meaningful NRTA as otherwise the resolution for time-of-flight measurements of the transmission spectrum is insufficient. The sub-nanosecond initial pulse width of the laser-driven neutron pulses is a benefit over accelerator based neutron sources, which typically require substantial effort, such as a proton storage ring, to reach sub-microsecond pulse width.

Pioneering work by Priesmeyer & Harz was already conducted several decades ago [Priesmeyer 1975] and the technique, while not often applied to fuels, has matured [Schillebeckx 20012]. According to a detailed study by Chichester & Sterbentz [Chichester 2011a & 2011b], for efforts such as the Next

Generation Safeguards Initiative (NGSI), Neutron Resonance Transmission Analysis “may be a very capable experimental technique for spent fuel assay measurements”. In this study, a pulsed neutron source is identified as a requirement with a “raw accelerator neutron spectrum with an intensity prior to moderation of $>10^{12}$ n•s^{-1}“ as an estimated flux requirement. At the 80 J Trident laser, 10^{10} n/pulse were achieved without much optimization of target/moderator. Therefore, a 100 J laser operating at 10 Hz with an optimized target (promising gains by an order of magnitude), utilizing the fact that with deuteron break-up the majority of neutrons can be captured in a moderator, could already fulfil the requirements for this particular application. Furthermore, the compactness of laser-drive sources may allow to provide such an inspection system transportable by truck, allowing e.g. nuclear forensics.

An extension of this resonance technique is the determination of the absorption line width in an energy spectrum. The Doppler broadened absorption width is directly correlated to the thermal motion and therefore the sample temperature. As demonstrated by Yuan, an absorption line can be detected in a single shot experiment [Yuan 2005]. The travel time through the sample for the neutrons covering the energy range of the resonance used for the broadening analysis defines the measurement time for this temperature probe (e.g. a few hundred ns). This technique can be used to measure the bulk temperature of a transient sample, e.g. in high energy density experiments. As demonstrated by [Yuan 2005] for high-explosive induced shock in metal, temperature uncertainties of 50K can be achieved in such single shot experiments. Such diagnostic may be of interest for the TREAT reactor at INL, allowing to measure true bulk temperature. As demonstrated by [Stone 2005a & 2005b] in the static case, i.e. with thousands of neutron pulses accumulated to improve statistics, this technique can be used to measure bulk temperature without a sensor in harsh environments (a high pressure cell in their case). For the DOE/NE mission, this could be applied to measure the temperature in samples not accessible for other means of thermometry (thermocouples, pyrometry), e.g. in temperature studies.

Epithermal neutrons (0.4 eV to 500 keV) in conjunction with a spatially resolved time-of-flight detector are utilized for energy-resolved neutron imaging as demonstrated and applied to nuclear fuels in various other reports from our group (see e.g. Figure 2 and Figure 3). Again, the order of magnitude lower flux can be partially compensated by exploiting the ability to move the sample/detector much closer to a compact laser-driven neutron source than is possible at LANSCE. This would allow spatially resolved CT of the densities of various isotopes present in a sample (e.g. uranium or plutonium isotopes) at comparable count times as feasible at LANSCE, e.g. few days for a full tomography dataset. The pulse structure and the ability to conduct this with several cm of Pb between sample and detector would allow to much better discriminate against gamma background from a highly radioactive sample than is possible with a reactor based constant source. For resonances at higher neutron energies, typically not accessible for imaging due to flux/pixel, non-spatially resolved neutron transmission resonance analysis (NTRA) could be employed since the pulses of <1ns will provide benefits: For a flightpath length of 20m (approximately the length of the DANCE instrument at LANSCE, dedicated to cross-section measurements), a pulse width of ~270 ns (the standard pulse width at LANSCE’s target 1) results in a 1.9% contribution of the initial pulse width to the resolution for resonance measurements at 10 keV neutron energy. For the ~1 ns pulse width provided by a laser-driven neutron source, this contribution would drop to 0.007%, making the initial pulse width practically negligible for cross-section measurements. This is an immediate benefit provided by laser-driven sources for NRTA applied to nuclear fuel assay since the entire neutron pulses are useful without any further beam conditioning, e.g. choppers, or efforts to condense the original ion pulses, as is the case with the proton storage ring at LANSCE, which adds considerable complexity to the operation. Instrumentation cost for NRTA would be considerably less than $100k (e.g. photomultiplier tubes with scintillator and associated data acquisition), while a setup for time-of-flight imaging at LANSCE would be in excess of $100k.

8.4 MeV neutron and X-ray Flash Radiography

At LANSCE, in the past few years radiography with unmoderated neutrons (1 MeV < E_n < 100 MeV) was developed, adding yet another contrast mechanism to the cold, thermal, and epi-thermal neutron energies. While this capability was not yet applied to e.g. nuclear fuel pellets, the high penetration possible with this type of radiation adds yet another tool. The compact, accessible laser-driven neutron source would allow by a simple on-the-fly target change to an unmoderated target (or removal of the moderator around the Be target) and, to characterize a sample with this probe. While likely also the detector, or at least the scintillator screen, would need to be changed, such change could possibly done even without moving the sample. This truly would make such a source a multi-probe characterization tool, well suited for DOE/NE mission relevant characterization of e.g. new fuel forms. Due to the short pulse duration, with a short shutter time of the detector, and the ability to penetrate centimeters of Pb, the radiation emitted from a highly radioactive sample would be manageable. In particular for materials that also contain hydrogeneous materials, blocking thermal and epi-thermal neutrons, this technique will have benefits.

To explore this potential, a Perkin Elmer 40 cm (diagonal) amorphous Si detector system used at the unmoderated target 4 at LANSCE was installed at Trident in a setup with only the Be target for neutron converstion, but no moderator. The results of a single pulse exposure are shown in Figure 21.

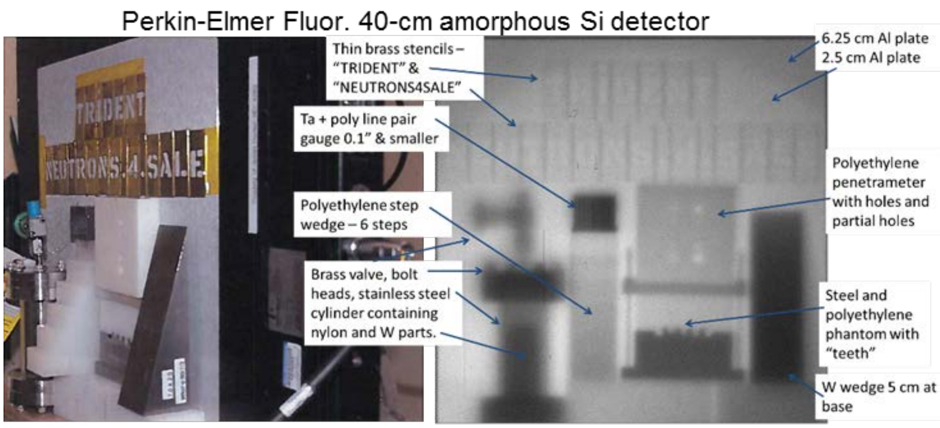

Figure 21: Photograph of the setup for demonstration experiment at the Trident source (left) and single pulse radiograph (right). The attenuation of the polyethylene step wedge in the bottom left indicates that the radiation is predominantly neutrons (Radiograph courtesy of R. Nelson & J. Hunter/LANL).

Utilizing laser-accelerated electrons instead of deuterons, e.g. with the laser pulse hitting a conventional plastic target, and using a ~0.5 mm thick tantalum disk as beamstop or catcher target, the decelerated electrons emit bremsstrahlung peaked at 2 MeV, i.e. very hard X-rays [Fernandez 2017]. These also have high penetration power for high Z materials such as nuclear fuels and due to the interaction with the electronic shell rather than the nuclei provide yet another contrast mechanism for imaging. Again, changing the source from thermal/epi-thermal neutrons to high energy neutrons to high energy X-rays can be done in an appropriately designed target setup with e.g. a highly radioactive sample in place, minimizing handling of such samples. In the last campaign at Trident, the ability to produce very hard X-ray beams was explored. Radiographs of a tungsten kaleidoscope of the U.K. Atomic Weapons Establishment (AWE), allowed to determine the source-size of Trident produced laser-driven hard X-ray single shot radiography (Figure 22). The pixel size of the detector turned out to be the limiting factor of this exercise and only an upper limit of 125 μm for the source size could be established. For comparison, the same kaleidoscope measured at the Dual Axis Radiographic Hydrodynamic Test facility (DARHT) at LANL, using a conventional electron linear accelerator and a 19 mm cathode to produce hard X-rays, has a source size of 750 μm. This makes the laser-driven hard X-ray source an excellent tool for imaging applications, especially for dynamic processes due to the short pulse (flash radiography). A source size for high energy neutrons has not yet been determined, but since the proton and deuteron beams impinging on the targets have similar characteristics, a similarly small source size can be expected.

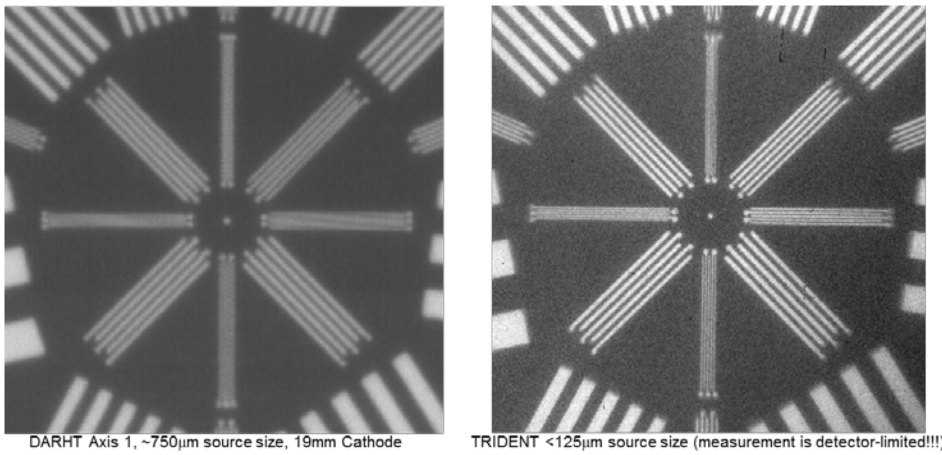

Figure 22: Comparison of an AWE tungsten kaleidoscope used to determine resolution in radiography experiments. On the left, a radiograph from the Dual Axis Radiographic Hydrodynamic (DARHT) facility is shown. On the right, the same target is shown with a radiograph measured at Trident (Radiographs courtesy of R. Nelson & J. Hunter/LANL).

8.5 Protons for material characterization

At LANSCE, 800 MeV protons are used as a probe to characterize materials. While neutrons and X-rays cannot be focused in practical applications, the charge of the protons allows to build magnetic lenses to implement magnification similar to an electron microscope [Aufderheide 1999]. Figure 23 shows a comparison of radiographs of the same rodlet containing Urania fuel pellets with purposefully introduced voids and tungsten pieces of different sizes obtained with different probes. Protons provide a contrast mechanism similar to X-rays as they interact with the charge of the atoms.

While certainly more effort than neutron and X-ray imaging discussed so far, the ability of protons with energies above 100 MeV to penetrate containers and high Z materials like nuclear fuels, the ability to utilize magnifiers as developed at pRAD at LANSCE to zoom into details within e.g. an irradiated fuel non-destructively is attractive.

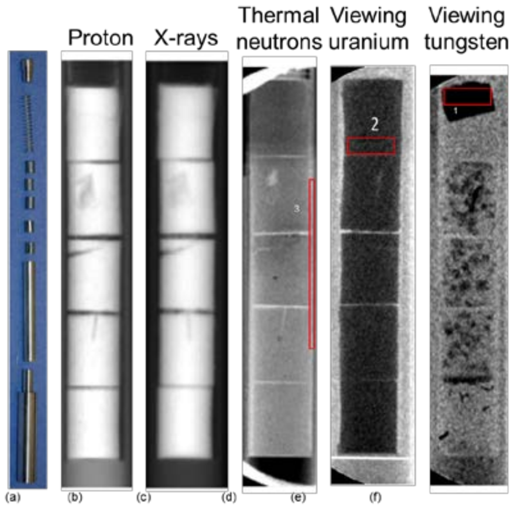

Figure 23: Comparison of mock-up fuel pellets used in [Morris 2013] and [Tremsin 2013]. The pellets contained purposefully introduced flaws and tungsten inclusions, which are only visualized by the energy-resolved epi-thermal neutron imaging.

8.6 Isotope production and proton irradiation

The Isotope Production Facility (IPF) at LANSCE is one of two facilities in the U.S. producing isotopes such as Strontium-182 or Germanium-168, and the LANSCE overall run cycle is dictated by the requirement to ensure a continuous supply between these two sources. The proton current utilized for this operation is 250 μA with a proton energy of 100 MeV. Even a lower proton flux would allow to de-centralize the production and save precious time for shipping, a race against the half-lives of the produced isotopes. Potentially the use of isotopes with even shorter half-lives may become possible if a laser-driven isotope production is located directly in a hospital. Depending on the cross-sections of the proton interaction processes with the target material, lower energies than the 100 MeV presently used may be sufficient. At present, alternative technologies for isotope production are cyclotrons, including super-conducting cyclotrons with proton acceleration energies of 100 MeV or more. Such devices are available commercially and operate relatively robustly.

At present, the number of protons accelerated to ~20 MeV with a laser-driven source is $\sim 4\times 10^{13}$ particles, i.e. protons and carbon nuclei in a plastic target or ~40μA at a 10 Hz operation. With optimizations of the laser-driven proton source for this particular applications, currents of ~100μA should be feasible, such that a 100 Hz laser-driven system should comfortably reach the 250 μA reached at LANSCE. While isotope production with laser-driven sources is feasible, a pulsed operation is not required for this particular application and the competition of cyclotrons makes this application less attractive for laser-driven systems.

9. Comparison to the field

A summary of the presently achieved parameters with laser-driven neutrons is compared to existing neutron sources in the tables below.

Parameter	*Parameter Range/Comment*						
Neutron source type	Laser-driven neutron source	Lujan Center (LANSCE)	low energy (4MeV) RFQ (LLNL)	OERLA (ORNL)	LENS (Indiana University)	D-T plasma tube	Dense Plasma Focus (DPF)
Spectrum	Thermal to ~10 MeV Energy spread 100 %	Thermal to >100 MeV	2.5- 6.54 MeV		Thermal to 10 MeV	2.5 MeV or 14 MeV (DD or DT fusion)	2.5 MeV or 14 MeV dependent on DD or DT
Neutrons per pulse	> 10^{10}/sr (equivalent to 2×10^{11} in 4π) [Roth 2013]	~6×10^{14} (@100 μA proton current)	5×10^9 n/s for 100 mA current (exit of collimator) [Hall 2007]	10^{11}	2×10^{10} for 5 μs pulses	simple units limited to 10^{10} n/s (DT) 10^8n/s (DD) [Buffler 2010]	10^{13} at 3 MA current (Gemini) with DT
Spatial Distribution	Isotropic component & four fold enhanced forward beam	Isotropic		Biased in forward direction	Biased in forward direction		
Opening angle	~90°	4π		~90º	~90º		
Neutrons reaching moderator	2×10^{10} /sr	~$3\text{-}6\times10^{12}$ (5-10% in current target 1 configuration)		10^{11}	2×10^{10}		
Initial pulse width	<1 ns	270 ns	Constant current	4-30 ns	5-1200 μs	μs pulses	few ns, but jitter and multiple pulses
Repetition rate	equals laser driver rate	20 Hz		12-1000 Hz	20-100 Hz	5 KHz	
Neutron Generation Scheme	Pitcher (deuterized plastic) + catcher (Be) + W reflector	Proton accelerator-driven, split tungsten target spallation neutron source		Electrons on Ta, Be targets	(p,n) on Be target		
Efficiency	>10^{-2}						

Co-moving particles	e^- (MeV), γ (MeV), ions (depending on thickness of converter)	p (<800 MeV), γ (MeV)			
Target	Thin, free standing foil (200 to 800 nm thick)	Ta-clad tungsten, ~10cm ∅, 20 cm long		Ta, Be	Be
Target/moderator dimensions	5 cm ∅, 5 cm long	60 cm ∅, 300 cm long [Mocko2013]			
Laser Parameters					
Energy	80J				
Pulse length	500 fs				
Contrast	$>10^{10}$				
Spot size	>5 μm				
Incident Angle	normal (10°)				

Table 1: Comparison of different neutron sources.

10. Other Applications

The applications for a laser driven neutron source are numerous. Because the laser driver can be made compact and mobile, for the first time a neutron source can by brought to users for various applications requiring pulsed neutron sources with intensity approaching that of neutron user facilities. At present most of the laser systems used in neutron production are large-scale systems designed for basic science; whereas, future systems will be designed for compactness and transportability so that they can fit onto a truck or trailer. Because the infrared laser and the optical transport lines are non-hazardous with respect to radiation safety, only the small target area needs to be shielded and, because of the absence of fission products in the deuterium break-up on beryllium, only during operation. Thus, the entire system is safe for transport and operation.

Moreover the short pulse duration affords excellent neutron energy resolution in time-of-flight measurements, and the high peak brightness allows for gated detector systems that can improve the signal to noise ratio and facilitate monitoring lower total neutron numbers and physical dimensions in applications. Presented in what follows are a few application examples for laser driven neutrons that are presently at the edge of technical readiness.

10.1 Fast neutron radiography

This technique has already been demonstrated using the LANL Trident laser in 2012 [Roth 2013]. MeV neutrons from the laser driven source were used to obtain radiographs of a test object made with tungsten blocks of different thickness (see Figure 24). Because neutron interactions with materials are distinct from X-ray interactions, they both can probe an object and provide complementary information. With gated detection one can chose for observation the energy range of the neutrons taking advantage of energy-dependent differences in neutron scattering and absorption in different elements. Thus materials can be identified. An example is given in [Jung 2013a] for neutrons between 2.5 and 15 MeV.

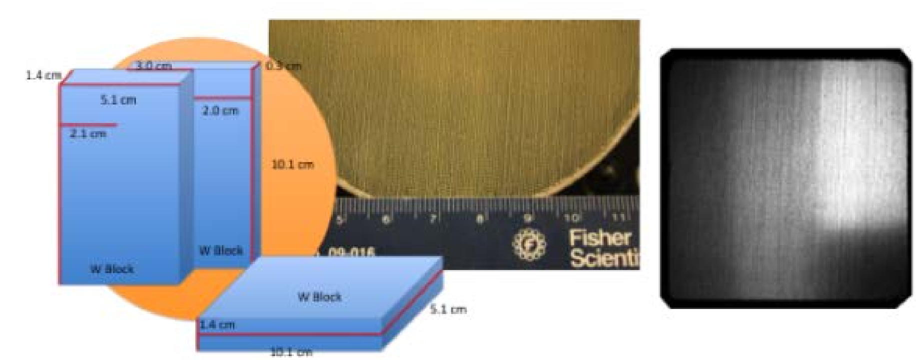

Figure 24: Example of laser-driven fast neutron radiography. The tungsten blocks in front of the detector result in absorption and scattering of the neutrons shown in intensity variations in the scintillating fiber detector. This image was taken without neutron energy selection (in contrast to [Roth 2013])

Besides its compactness, another advantage of a laser-driven neutron source is the directionality of the energetic neutrons. This also minimizes the need for shielding during the imaging. This flash high E neutron radiography, which is accompanied by a sub-nanosecond high E (MeV) γ flash, allows to visualize transient phenomena. DOE/NE mission relevant application may be the TREAT reactor.

10.2 Active Interrogation of Sensitive Nuclear Material

One of the most feared threats for modern societies is the uncontrolled proliferation of sensitive nuclear material and the possibility of a nuclear terrorist attack. Laser-driven neutron beams have been demonstrated to penetrate deeply into shielded containers and excite nuclear reactions in fissile material resulting in detectable fission neutrons. Both prompt and delayed neutron emission has been measured at the LANL Trident laser and the signal to noise ratio was high enough to allow for a large stand-off distance (distance between the source, the container to be probed and the detector assembly) and good threat discrimination [Favalli 2016].

10.3 On-site neutron based system tests

Neutrons are used in a variety of technical applications, e.g. in oil and drilling industry [Schultz 1985], or in identifying structural defects. One example is testing turbine blade defects for aircraft engines [Thornton 2003]. A compact laser-driven neutron source that might fit into a vehicle (as with mobile laser peening laser systems), could be envisioned as a mobile testing facility for jet engines. Colleagues in Japan have proposed testing the metal internal structure of bridges nationwide for corrosion using a mobile (laser-driven) neutron source to determine the need and urgency for repair [Seki 2014].

For the DOE/NE mission, availability of compact laser-driven sources with investment costs of less than $10M could make pulsed neutron characterization a tool for novel reactor design (e.g. an in-process measurement of the enrichment level or fuel composition using NRTA) or advanced fuel forms. Similar to current neutron sources utilized to verify enrichment levels by attenuation of a constant beam from a radioactive neutron source during fabrication, laser-driven pulsed neutron sources could become a tool for quality control in fuel fabrication plants. The development of commercially available in-house synchrotron sources [Lyncean 2016] may serve as an example how rapidly such developments may occur if the component price lends itself to economic sales numbers.

10.4 Radiation Damage Research

Neutron impact in material is known to cause lattice damage by replacing and shifting atoms from their initial positions. This phenomenon is measured as DPA (displacement per atom) and is a crucial measure of the lifetime and stability of material exposed to neutron fluxes (such as materials in fission reactors and fusion devices in the future). However, it is known that the majority of neutron-induced defects are not detectable after long-term exposures and the annealing of defects plays an important role in real material behavior. The underlying physics, timescales and dependences on initial conditions (stress, temperature) are poorly understood. One challenge in research is to observe the damage and recovery on timescales shorter than the ones set by the diffusion of the displaced atoms (within a few ns). An intense, sub-ns neutron source coupled to high-resolution x-ray diffraction diagnostics (e.g. an X-ray free electron laser) could, for the first time explore the mechanism leading to damage and annealing.

Obviously this field is relevant to the DOE/NE mission. Estimates for the 20 Hz LANSCE spallation source for an irradiation specimen placed above the tungsten target indicated that 0.1-0.2 dpa could be expected within a 6 months exposure time, significantly lower dpa than in the ATR. However, this type of neutron sources may still enable irradiation experiments e.g. in an academic environment (see below). Besides the ability to utilize a laser-driven pulsed neutron source in the vicinity of the ATR, a laser-driven neutron source with its compact and accessible target could be operated at a higher repetition rate (kHz) than the 10-20 Hz required for time-of-flight methods for a certain period to irradiate, then switched to characterization mode to investigate the early stages of radiation damage. The comparably easy access to the forward directed neutrons allows to re-gain an order of magnitude in neutrons on sample compared to the LANSCE estimate even if the laser-driven source is weaker. Temperature control and other probes are also easier installed in the vicinity of a laser-driven neutron source compared to the LANSCE target. The benefit of laser-driven neutron sources for this particular application may lay in the ability to design the neutron source for the irradiation experiment rather than the need to design an irradiation experiment for an existing neutron source.

10.5 Academic Access

Many disciplines could benefit from a compact neutron source. Examples include biology, material sciences, geology, and of course physics. Only a few universities in the world can have direct access to a large-scale spallation facility or an on-campus nuclear reactor and even then the access is limited and involves complicated procedures to avoid contamination or exposure to radiation. The benefit of a laser-driven neutron source is the safety of the laser system itself; although a class 4 laser system is operating a near infrared beam that must propagate up to the entrance of a compact target chamber, there is no radiation hazard from the laser. Also fast, safe access is possible after experiments because the intense neutron pulse is only present during an experiment in operation with no radioactive fission products in the neutron target, making the potential sample activation the only radiation risk. Moreover the directionality of the neutron beam allows for beam guiding to the experiment that avoids unnecessary exposure to radiation. An affordable, compact short pulse laser is within the budget of most universities and the number of such systems is growing (e.g. throughout Europe), making such systems in conjunction with the radiation safety much more similar to advanced X-ray tubes or electron microscopes. Compact laser driven neutron sources could broaden the academic access and therefore boost neutron related sciences in academia.

From the perspective of the DOE/NE mission, academic access to these tools provides training of researchers in nuclear engineering in advanced characterization techniques applicable to materials relevant to DOE/NE, e.g. fuels or irradiated structural materials. The crystallography of uranium-based phases is much more accurately determined with neutrons [Reiche 2016] and if university groups dealing with research in uranium-nitrides, -silicides, -borides etc. would have in-house access to a small neutron diffractometer, similar to having an X-ray diffractometer, research in thermal behavior, phase diagrams, microstructure evolution etc. would significantly accelerate development of fuel forms based on these phases.

11. World-wide Research Activities in Laser-driven Neutron Sources

Existence of a world-wide community engaged in making laser-driven neutron sources a reality is not only testament of the relevance of this technology, but also ensures that progress is made. In the U.S., research efforts in laser-driven particle acceleration are for example undertaken at LLNL for the National Ignition Facility (NIF), at the Texas Petawatt Facility for proton acceleration and wakefield electron acceleration (similar to synchrotron sources), and at the Nevada Terawatt Facility, where laser-driven gamma bursts are used for flash-radiography of laser-generated plasma. At LANL, where several milestones in the development of this technique were accomplished, the Trident laser was recently retired with a plan to transfer it to the Texas Petawatt Facility. In Europe, ultra-intense laser facilities exist for instance at GSI, with the petawatt Phelix laser, or at the British Atomic Weapons Establishment (AWE) with the Orion laser facility [Hopps 2013]. A European funded research infrastructure for laser-based research user facilities, the Extreme Light Infrastructure (ELI), is almost finalizing construction at three locations (with a fourth planned). Of particular interest for the topic of this report, is the ELI-Beamlines facility near Prague with a research focus on secondary radiation and particles, scheduled to start operations in 2018. As can be seen in Figure 15, the ELI laser is designed to reach neutron intensities similar to the LANSCE neutron pulses. The total budget for this facility, including four lasers, buildings, clean rooms and related infra-structure, is

278 million Euros (~$300M). For comparison, the budget for the Spallation Neutron Source at ORNL, was $1.4B, with the majority of that budget consumed by the accelerator.

Some of the lasers for the ELI Beamlines facility are purchased commercially from companies such as Thales Optronique (TOSA, France) or National Energetics (U.S.A.), underlining that the technical maturity of the field is beyond R&D demonstrations and that markets for suitable lasers exist.

Conferences are organized in the field with a particular focus or special sessions on neutron production, such as the first Nuclear Photonics Conference, held in October 2016 in Monterey (with the next one planned for 2018 in Romania), or the first Conference on Laser and Accelerator Neutron Sources and Applications (LANSA) in Yokohama, Japan.

Figure 25: Conference attendees of the Nuclear Photonics conference in Monterey, CA, October 2016. Several authors of this report were in the attendance, author M. Roth served as program chair for the conference.

At the Nuclear Research Center Jülich, Germany, the concept of the Jülich high-brilliance neutron source project was recently started [Rucker 2016]. While not based on laser-driven neutron sources, it promotes the use of deuteron break-up as the mode of neutron production and thus designs target/moderator systems for the same pre-dominantly forward travelling neutron pulses. Because of the use of conventional accelerators, the neutron pulse width is far broader than the sub-nanosecond pulses possible with laser-driven sources. However, the efforts in this project for design and testing of target/moderator systems specifically designed for this neutron production mechanisms provide the potential for synergy, thus accelerating the development of the first laser-driven pulsed neutron source for production. Similarly, the Japan Collaboration on Accelerator-driven Neutron Sources [JCANS 2016], a network of currently nine accelerator-driven neutron sources (five in operation, four under construction) is actively optimizing target/moderator systems for compact neutron sources.

All of these activities underline the significant research efforts world-wide by an active community working towards making a production laser-driven pulsed neutron source a reality.

12. Summary and Outlook

We described the underlying physics of laser-driven neutron sources, the state of the art in high power short pulse laser systems, a system for a continuous target feed, as well as potential applications and the existing community. While not covered in this report, models and diagnostics for this particular application exist and continue to be developed (see e.g. [Fernandez 2017] for more details). With discovery only ten years ago of the break-out afterburner (BOA) effect, accelerating the particles about five times more when an appropriate laser pulse shape can be accomplished, coupled with the advancements in laser and laser-optics driven by a multitude of other applications, a production laser-driven intense pulsed neutron source can be envisioned.

While it is clear that pulsed neutron sources provide great benefit for characterization of fresh as well as irradiated or spent nuclear fuels, suitable neutron sources so far were with investment cost of more than 1 billion dollar far too expensive to be installed e.g. at the ATR at INL. As outlaid in this report, laser-driven neutron sources may be able to deliver similar flux on sample at a cost of several ten million dollar. This would bring the investment for such a characterization tool closer to e.g. a TRIGA reactor. Conventional electron or proton accelerator based neutron sources, such as ORELA at ORNL [ORELA 2017] and the LENS source at Indiana University [LENS 2017], utilize similar processes for neutron generation (i.e. (p,n) reactions on targets such as Be) but are limited by the extraction of electrons or protons from the electron/ion source to ~100 mA peak current. In order to increase the neutron production with these sources either the particle energy has to be increased or components such as storage rings have to be installed, driving the cost quickly towards those of spallation sources.

The fundamentally different particle acceleration mechanism with the laser circumvents these limitations. Even though the total number of neutrons produced with a laser pulse today is significantly lower than at a spallation neutron source (with today's most powerful lasers not yet tested for neutron production, see Figure 15), the flux on sample is already comparable for some applications. The main reasons for this are firstly, that almost all neutrons produced by deuteron break-up reaction reach the moderator (while in a spallation source only 5-10% of the produced neutrons reach a given moderator), providing about one order of magnitude gain compared to the LANSCE target. Secondly, the compactness of the target/moderator system (~5 cm diameter, 5 cm long cylinder plus Pb shielding for gammas viz. e.g. the 60 cm diameter, 300 cm long target/moderator system of LANSCE [Mocko 2013] with a 4.5 m radius concrete bulk shield) will allow source to sample distances of as little as L=1 m viz. L=~6m at LANSCE, allowing more than an order of magnitude increase in flux on sample, which is directly usable for imaging applications. The compactness of the target will also allow to change the target from a thermal neutron target to an unmoderated high energy/fast neutron target as well as to a high energy (MeV) X-ray target, producing high intensity high energy bremsstrahlung from decelerating electrons. As was demonstrated in the past year at Trident, for imaging applications the intensity provided in a single pulse is sufficient with an unparalleled small source size of 100 μm or less, directly affecting resolution. With sub-nanosecond intense high energy gamma radiography even characterization of highly radioactive materials should be possible since only a nanosecond shutter time on the imaging equipment is required, allowing the radiation from the imaging source to greatly exceed the contribution from radioactive decay.

In summary, with laser-driven neutron sources LANSCE-like neutron-based characterization capabilities plus high energy X-ray radiography, both probing the bulk of irradiated materials, can be potentially deployed pool-side at ATR. As demonstrated at LANSCE, such characterization would allow to fully characterize capsules prior to irradiation and identify irregularities in fully encapsulated materials after irradiation over a vast parameter space, ranging from micro-structural parameters like texture and strain to chemical variations to voids and cracks. Identification of regions of interest would allow further detailed destructive evaluation with a well informed decision where to cut a given specimen. By maximizing the insight gained from irradiation experiments, the development and ultimately licensing of new fuel forms as well as structural materials can be significantly accelerated.

The immediate path forward towards deploying laser-driven LANSCE-like capabilities in support of the DOE/NE missions is for the LANL ANDE team to remain engaged in experimental activities, e.g. by supporting participation in campaigns at laser facilities aimed at optimizing neutron production or characterizing neutron and X-ray imaging applications. The LANL team supported by the ANDE work package has access to state-of-the-art neutron and X-ray imaging detectors as well as diffraction detectors, which would be otherwise unavailable to the experimental efforts at the laser sources. Participation of the LANL ANDE team therefore enhances the data produced during such campaigns while at the same time directly exploring and demonstrating the capabilities of laser-driven neutron sources for DOE/NE applications. Such activity would ensure continued engagement of DOE/NE funded staff with leaders in the community developing laser-driven neutron sources.

The next logical step towards a potential installation of a laser-driven LANSCE-like facility at e.g. INL would be a more detailed design study, informed by specific requirements of INL, for a system that could be installed within 5-7 years. The authors of this report span the required fields of expertise for such a conceptual study.

13. References

[Albright 2007] B. J. Albright et al., “Relativistic Buneman instability in the laser breakout afterburner”, Phys. Plasmas, **14**, p. 094502 (2007)

[Aufderheide 1999] M.B. Aufderheide III et al. AIP Conf. Proc. 497 (1999) 706–712.

[Alejo 2016] Alejo, A., et al. "Recent developments in the Thomson Parabola Spectrometer diagnostic for laser-driven multi-species ion sources." Journal of Instrumentation 11.10 (2016): C10005.

[Banerjee 2012] S. Banerjee et al. “High-efficiency 10 J diode pumped cryogenic gas cooled Yb:YAG multislab amplifier“, Optics Lett., **37**, p. 2175 (2012)

[Bahk 2004] S.-W. Bahk et al. “Generation and Characterization of the highest laser intensities (10^{22} W/cm^2)”, Optics Lett. **29**, p. 24 (2004)

[Bang 2013] W. Bang et al. “Experimental study of fusion neutron and proton yields produced by petawatt-laser-irradiated D2-3He or CD4-3He clustering gases“, Phys. Rev. E, **87**, p. 023106 (2013)

[Batha 2008] S. H. Batha et al. "Trident high-energy-density facility experimental capabilities and diagnostics," Rev Sci Instrum **79**, 10F305 (2008).

[Boot 1957] H. Boot and R.B.R. Shersby-Harvie, “Charged Particles in a non-uniform Radiofrequency field”, Nature, **180**, p. 1187 (1957)

[Borghesi 2006] M. Borghesi et al., “Fast Ion Generation by High- Intensity Laser Irradiation of Solid Targets and Applications“, Fusion Science and Technology, Vol. 49, **3**, p.412 (2006)

[Brunel 1987] F. Brunel “Not so resonant absorption”, Phys. Rev. Lett. **59**, p. 525 (1987)

[Buffler 2010] Buffler, A. and Tickner J. “Detecting contraband using neutrons: Challenges and future directions“, Radiation Measurements, **45**, p.1186 (2010)

[Busold 2014] S. Busold et al., “Commissioning of a compact laser-based proton beam line for high intensity bunches around 10 MeV” Phys. Rev. ST-AB, **17**, p. 031302 (2014)

[Chichester 2009] D.L. Chichester, “Production and Applications of Neutrons Using Particle Accelerators”, INL report INL/EXT-09-17312.

[Chichester 2011a] D.L. Chichester, J.W. Sterbentz, „Neutron Resonance Transmission Analysis (NRTA): Initial Studies of a Method for Assaying Plutonium in Spent Fuel“, INL report INL/CON-10-20684, 2011.

[Chichester 2011b] D.L. Chichester, J.W. Sterbentz, “A Second Look at Neutron Resonance Transmission Analysis as a Spent Fuel NDA Technique”, INL report INL/CON-11-20783, 2011.

[Cowan 2000] T.E. Cowan et al.,„Photonuclear Fission from High Energy Electrons from Ultraintense“ Laser-Solid Interactions**“,** Phys. Rev. Lett., **84**, p.903 (2000)

[Cowan 2004] T.E. Cowan et al., "Ultra-low emittance, multi-MeV proton beams from a laser virtual-cathode plasma accelerator", Phys. Rev. Lett., **92**, p. 204801 (2004)

[Crane 2010] Crane, J. K., et al. "Progress on converting a NIF quad to eight, petawatt beams for advanced radiography." Journal of Physics: Conference Series. Vol. 244. No. 3. IOP Publishing, (2010).

[CSNS 2017] China Spallation Neutron Source website http://csns.ihep.ac.cn/english/Introduction/Introduction.htm

[Danson 2014] C. Danson et al., "Petawatt class lasers worldwide", High Power Laser Science and Engin., **3**, p. e13 (2015)

[Dawson 2012] Dawson, Jay W., et al. "High average power lasers for future particle accelerators." AIP Conference Proceedings. Vol. 1507. No. 1. AIP, (2012).

[Day 2011] C. Day, "Is there something wrong with the Spallation Neutron Source?", Physics Today, DOI:10.1063/PT.5.010133.

[Ditmire 1999] T. Ditmire et al., „Nuclear fusion from explosions of femtosecond laser-heated deuterium clusters", Nature, **398**, p.489-492 (1999)

[Doria 2012] D. Doria et al., "Biological effectiveness on live cells of laser driven protons at dose rates exceeding 10^9 Gy/s", AIP Advances, **2**, p. 011209 (2012)

[ELI 2011] ELI – Extreme Light Infrastructure - White book, http://cswiki.eli-beams.eu/public/ELI_White_Book092010.pdf

[ELI2012] http://www.esfri.eu/success-stories/extreme-light-infrastructure-when-scientific-excellence-contributes-europe%E2%80%99s

[ESS 2014] ESS Construction Phase Cost Book 2014, available on-line at https://europeanspallationsource.se/sites/default/files/ess_cost_book_2014_2_blank.pdf

[Favalli 2016] Favalli, Andrea, Nevzat Guler, Daniela Henzlova, Katerina Falk, Stephen Croft, Donald C. Gautier, Kiril D. Ianakiev et al. "Experimental observation of $\ beta $-delayed neutrons from $^{9} $ Li as a way to study short-pulse laser-driven deuteron production." arXiv preprint arXiv:1605.05702 (2016).

[Fernandez 2014] J. C. Fernandez et al., "Fast ignition with laser-driven proton and ion beams", Nucl. Fusion, **54**, p. 054006 (2014)

[Fernandez 2017] J. C. Fernandez et al., „Laser-plasmas in the relativistic-transparency regime: science and applications", to be published in Physics of Plasmas (2017).

[Fletcher 2016] L. B. Fletcher et al., "High resolution x-ray Thomson scattering measurements from cryogenic hydrogen gets using the linac coherent light source", Review of Scientific Instruments 87, 11E524 (2016).

[Fonseca 2002] Fonseca, R., et al. "OSIRIS: a three-dimensional, fully relativistic particle in cell code for modeling plasma based accelerators." Computational Science—ICCS 2002 (2002): 342-351.

[Gan 2017] Gan, Z. et al. 200 J high efficiency Ti:sapphire chirped pulse amplifier pumped by temporal dual-pulse. Opt. Express 25, 5169–5178 (2017).

[Gauthier 2016] M. Gauthier et al., "High-intensity laser-accelerated ion beam produced from cryogenic micro-jet target" Review of Scientific Instrumnets 87, 11D827 (2016)

[Guenther 2011] Günther, M. M., et al. "A novel nuclear pyrometry for the characterization of high-energy bremsstrahlung and electrons produced in relativistic laser-plasma interactions." Physics of Plasmas 18.8 (2011): 083102..

[Guenther 2012] M. Guenther et al. „Development of High-Power Laser Based Nuclear Applications", Fus. Sci. and Technol., Vol 61, **1**, p. 231-236 (2012)

[Hall 2007] J. M. Hall et al., "The Nuclear Car Wash: Neutron interrogation of cargo containers to detect hidden SNM", Nucl. Instr. and Meth. B, **261**, p. 337 (2007)

[Hatchett 2000] S. Hatchett et al., "Electron, photon, and ion beams from the relativistic interaction of Petawatt laser pulses with solid targets", Phys. Plasmas **5**, p. 2076 (2000)

[Hegelich 2002] B.M. Hegelich et al., "MeV Ion Jets from Short-Pulse-Laser Interaction with Thin Foils", Phys. Rev. Lett., **89**, Vol. 8, p. 085002 (2002)

[Hegelich 2005] B.M. Hegelich et al., "Spectral properties of laser-accelerated mid Z-MeV/u ion beams", Phys. Plasmas, **12**, p. 056314 (2005)

[Hegelich 2011] B.M. Hegelich et al., "Experimental demonstration of particle energy, conversion efficiency and spectral shape required for ion-based fast ignition", Nucl. Fusion, **51**, p. 083011 (2011)

[Higginson 2010] D.P. Higginson et al., "Laser generated neutron source for neutron resonance spectroscopy", Phys. Plasmas, **17**, p. 100701 (2010)

[Higginson 2011] D.P. Higginson et al. „Production of neutrons up to 18 MeV in high-intensity, short-pulse laser matter interactions", Phys. Plasmas, **18**, p. 100703 (2011)

[Hopps 2013] Nicholas Hopps, Colin Danson, Stuart Duffield, David Egan, Stephen Elsmere, Mark Girling, Ewan Harvey, David Hillier, Michael Norman, Stefan Parker, Paul Treadwell, David Winter, and Thomas Bett, "Overview of laser systems for the Orion facility at the AWE," Appl. Opt. **52**, 3597-3607 (2013)

[Hurriane 2014] O. Hurricane et al., "Fuel gain exceeding unity in an inertially confined fusion implosion" *Nature* **506**, p. 343–348 (2014)

[IAE04] IAEA-TECDOC-1439, Development opportunities for small scale accelerator driven neutron sources, Report of a technical meeting, Vienna, 18-21 May 2004

[Ino 2004] T. Ino et al., “Measurement ofneutron beam characteristics at the Manuel Lujan Jr. neutron scattering center”, Nuclear Instruments and Methods in Physics Research A 525 (2004) 496–510

[JCANS 2016] http://phi.phys.nagoya-u.ac.jp/JCANS/

[Jung 2013] D. Jung et al., “Efficient carbon ion beam generation from laser-driven volume acceleration“, New Journal of Physics, **15**, p. 023007 (2013)

[Jung 2013a] D. Jung et al. “Characterization of a novel, short pulse laser-driven neutron source“ Phys. Plasmas, **20**, p. 056706 (2013)

[Kar 2016] S. Kar et al., “Beamed neutron emission driven by laser accelerated light ions“ New Journal of Physics, **18**, p. 053002 (2016)

[Kim 2016] J. B. Kim, S. Goede, S. H. Glenzer, “Development of a cryogenic hydrogen microjet for high-intensity, high-repetition rate experiments”, Review of Scientific Instruments 87, 11E328 (2016)[Kimura 2011] S. Kimura and A. Bonasera, “Deuteron-induced reactions generated by intense lasers for PET isotope production”, Nucl. Instrum. And Meth. A, **637**, p. 164 (2011)

[Krygier 2015] A.G. Krygier et al. „Selective deuterium ion acceleration using the Vulcan petawatt laser“, Phys. Plasmas, **22**, p. 053102 2015

[Lancaster 2004] K. Lancaster et al. „Characterization of 7Li„p,n...7Be neutron yields from laser produced ion beams for fast neutron radiography“, Phys. Plasmas, Vol 11, p. 3404 (2004)

[Ledingham 2004] K.W.D. Ledinham et al., “High power laser production of short lived isotopes for positron emission tomography”, J. Phys. D: Appl. Phys., **37**, p. 2341 (2004)

[LENS 2017] http://www.indiana.edu/~radeff/abeam.html

[Lisowski 1990] P.W. Lisowski et al., “The Los Alamos National Laboratory Spallation Neutron Sources“, Nucl. Science and Engineering, **106**, p. 208 (1990)

[Lisowski 2006] P.W. Lisowski and K.F. Schoenberg „The Los Alamos Neutron Science Center“, Nucl. Instrum. and Meth. A, **562**, p. 910-914 (2006)

[Lyncean 2016] http://www.lynceantech.com/

[Macchi 2013] Macchi, A., et al.,”Ion acceleration by superintense laser-plasma interaction”, Review of Modern Physics, **85** 751 (2013).

[Maksimchuk 2013] A. Maksimchuk et al. “Dominant deuteron acceleration with a high-intensity laser for isotope production and neutron generation“, Appl. Phys. Lett., **102**, p. 191117 (2013)

[Maiman 1960] T.H. Maiman, “Stimulated optical radiation in ruby”, Nature, **187**, p. 493-494 (1960)

[Malka 2004] V. Malka et al., “Practicability of proton therapy using compact laser systems”, Med. Phys., **31**, p. 1587 (2004)

[Mocko 2013] Mocko, M., G. Muhrer. "Fourth-generation spallation neutron target-moderator-reflector-shield assembly at the Manuel Lujan Jr. neutron scattering center." Nuclear Instruments and Methods A704 (2013): 27-35.

[Morris 2013] C.L. Morris et al. “Qualitative comparison of bremsstrahlung X-rays and 800 MeV protons for tomography of urania fuel pellets”, Rev. Sci. Instrum. 84 (2013) 023902.

[Mourou 1985] D. Strickland and G. Mourou “Compression of amplified chirped optical pulses” Optics Communications, **56**, p. 219 (1985)

[Neumayer 2005] P. Neumayer et al. “Status of Phelix laser and first experiments“, Laser and Part. Beams, Vol.23, **3**, p. 385 (2005)

[Norreys 1998] P.A. Norreys et al., “Neutron production from picosecond laser irradiation of deuterated targets at intensities of 10^{19} W/cm^{2}“, Plasma Phys. and Control. Fusion, **40**, p. 175-182 (1998)

[Oppenheimer 1935]J.R. Oppenheimer and M. Phillips “Note on the Transmutation Function for Deuterons“, Phys. Rev. **48**, p.500 (1935)

[ORELA 2017] http://www.phy.ornl.gov/nuclear/orela/

[Papadopoulos 2016] D.N. Papapopousol et al., “The Apollon 10 PW Laser: Experimental and theoretical investigation of the temporal characteristics”, High Power Laser Science and Engin., **4**, p. e34 (2016)

[Patel 2003] P.K. Patel et al., “Isochoric Heating of Solid-Density Matter with an UltrafastProton Beams”, Phys. Rev. Lett. **91**, Vol.12, p. 125004 (2003)

[Perry 1999] M.D. Perry et al., “Petawatt laser pulses”, Opt. Letters **24**, p. 160 (1999)

[Pomerantz 2014] I. Pomerantz et al., “Ultrashort Pulsed Neutron Source“, Phys. Rev. Lett., **113**, p. 184801 (2014)

[Priesmeyer 1975] H.G. Priesmeyer & U. Harz, “Isotopic Assay in Irradiated Fuel by Neutron Resonance Analysis”, Atomkernenergie (ATKE) **25** (1975) 109-113

[Reiche 2016] H. M. Reiche et al., „In situ synthesis and characterization of uranium carbide using high temperature neutron diffraction”, Journal of Nuclear Materials, **471**, 308-316.

[Robinson 2008] A.P.L.Robinson et al., “Radiation pressure acceleration of thin foils with circularly polarized laser pulses”, New Journ. of Physics, **10**, p. 013021 (2008)

[Roth 2001] M. Roth et al., “Fast ignition by intense laser-accelerated proton beams”, Phys. Rev. Lett., **86**, p. 436 (2001)

[Roth 2002] M. Roth et al., “Energetic ions generated by laser pulses: A detailed study on target properties“, Phys. Rev. ST-AB, Vol. 5, p. 061301 (2002)

[Roth 2008] M. Roth, “Review on the current status and prospects of fast ignition in fusion targets driven by intense, laser generated proton beams”, Plasma Phys. And Contr. Fusion, **51**, p. 014004 (2008)

[Roth 2011] M. Roth, “The diagnostics of ultra-short pulse laser-produced plasma”, Journal of Instrum., **6**, p. R09110 (2011)

[Roth 2013] M. Roth, M. et al., “A bright, laser-neutron source based on relativistic transparency of solids“, Phys. Rev. Lett., **110**, p.044802 (2013)

[Rucker 2016] U. Rucker et al ., “The Jülich high-brilliance neutron source project” Eur. Phys. J. Plus (2016) 131: 19.

[Salamin 2008] Y.I. Salamin et al., “Direct High-Power Laser Acceleration of Ions for Medical Applications”, Phys. Rev. Lett., **100**, p. 155004 (2008)

[Schillebeeckx 2012] P Schillebeeckx et al., “Neutron resonance spectroscopy for the characterization of materials and objects”, Journal of Instrumentation **7.03** (2012): C03009.

[Seki 2014] Y. Seki et al., “A Simulation Study of Fast Neutron Imaging for Large-scale Concrete Structures“, Physics Procedia, **60**, p. 324 (2014)

[Shah 2009] R.C. Shah et al., “High-temporal contrast using low-gain optical parametric amplification”, Optics Lett., **34**, p. 2273 (2009)

[Schultz 1985] W.E. Schultz et al. “A borehole corrected pulsed neutron well logging system“ Nucl. Instrum. and Methods B, **10/11**, p. 1023 (1985)

[Snavely 2000] R.A. Snavely et al. “Intense High-Energy Proton Beams from Petawatt-Laser Irradiation of Solids“, Phys. Rev. Lett., **85**, p. 2945 (2000)

[SNS 2017] 42 USC §16320. Spallation Neutron Source (d) Authorization of appropriations (1) (1) Spallation Neutron Source Project

[Stone 2005a] H.J. Stone et al., “Remote determination ofsample temperature by neutron resonance spectroscopy”, Nuclear Instruments and Methods in Physics Research A 547 (2005) 601–615.

[Stone 2005b] H.J. Stone et al., “Temperature measurement in a Paris-Edinburgh cell by neutron resonance spectroscopy”, J. Appl. Phys. **98**, 064905 (2005).

[Sung 2016] J.H. Sung et al., “Development of 0.1 Hz 4.0 PW Laser at CoReLS”, Conference on Lasers and Electro-Optics, OSA Technical Digest (2016) (Optical Society of America, 2016)

[Tajima 1979] T. Tajima and J.M. Dawson, ” Laser electron accelerator”, Phys. Rev. Lett., **43**, p. 267 (1979)

[Tajima 2008] T. Tajima et al., “Laser acceleration of ions for radiation therapy”, Rev. of Acc. Science and Development, Vol1, p. 1 (2008)

[Thornton 2003] J. Thornton et al. “The Detection and sizing of flaws in components from the hot-end of Gas Turbines using phase-contrast radiography with neutrons: a feasibility study“, NDT&E International, **36**, p. 289 (2003)

[TUM 2015] https://www.tum.de/en/about-tum/news/press-releases/detail/article/32713/

[Tremsin 2013] A.S. Tremsin et al., „Non-destructive studies of fuel pellets by neutron resonance absorption radiography and thermal neutron radiography”, Journal of Nuclear Materials 440 (2013) 633–646.

[Vinogradov 2014] V.P. Vinogradov et al. ”Development and study of a portable plasma focus neutron source“ , Plasma Physics Reports, Vol. 40, No. 2, p. 146–159 (2014)

[Vogel 2013] S.C. Vogel, “A review of neutron scattering applications to nuclear materials”, ISRN Materials Science 2013 (2013).

[Vogel 2015a] S.C. Vogel et al., „Preliminary analysis of Advanced-PIE examination of ATF-1/LANL-1 encapsulated UN/U3Si5 composite and monolithic U3Si5 fuel rodlets”, LANL report LA-UR XXXX (2015).

[Vogel 2015b] S.C. Vogel et al., „Nondestructive characterization of fresh fuel using neutrons and path forward for measurement on irradiated rodlets”, LANL report LA-UR XXXX (2015).

[Vogel 2016a] S.C. Vogel et al., “Non-destructive Pre-irradiation Assessment of UN/U-Si LANL1 ATF formulation” LANL report LA-UR-16-27110 (2016).

[Vogel 2016b] S.C. Vogel et al., "Non destructive examination of UN/U-Si fuel pellets using neutrons (preliminary assessment)." LANL report LA-UR XXXX (2016).

[Vogel 2016c] S.C. Vogel et al., “Summary Report of Joint FCRD/NEAMS Technical Experts Working Meeting on Neutron-based NDE”, LANL report LA-UR XXXX (2016).

[Wagner 2014] F. Wagner et al. „”Pre-plasma formation in experiments using petawatt lasers“ Optics Express, Vol.22, **24**, p. 29505 (2014)

[Wagner 2016] F. Wagner et al. “Maximum Proton Energy above 85 MeV from the relativistic interaction of laser pulses with micrometer thick CH2 targets”, Phys. Rev. Lett. , **116**, 205002 (2016)

[Watanabe 2003] Watanabe, Noboru. "Neutronics of pulsed spallation neutron sources." Reports on Progress in Physics 66.3 (2003): 339.

[Wilks 1992] S.C. Wilks et al. “Absorption of Ultra-Intense Laser Pulses“, Phys. Rev. Lett., **69**, p.1383 (1992)

[Wilks 2001] S.C. Wilks et al., “Energetic proton generation in ultra-intense laser-solid interactions”, Phys. Plasmas **8**, p. 542 (2001)

[Windsor 1981] Windsor, C. "Pulsed Neutron Scattering, 1981." Taylor & Francis.

[Yin 2006] Yin, L. et al., „GeV laser ion acceleration from ultrathin targets: The laser break-out afterburner“, Laser and Part. Beams, Vol 24, **2**, p. 291-298 (2006)

[Yin 2007] Yin, L. et al. „Monoenergetic and GeV ion acceleration from the laser breakout afterburner using ultrathin targets“, Phys. Plasmas, **14**, p.056706 (2007)

[Yuan 2005] V.W. Yuan et al., “Shock Temperature Measurement Using Neutron Resonance Spectroscopy”, Phys. Rev. Lett. **94** 125504 (2005).

[Zou 2015] J.P. Zou et al. „High Power Laser Science and Engineering Design and current progress of the Apollon 10 PW project”, High Power Laser Science and Engineering, Vol 3, p. e2 (2015)

[Zulick 2013] C. Zulick et al., “Energetic neutron beams generated from femtosecond laser plasma interactions” Appl. Phys. Lett., **102**, p. 124101 (2013)